AD-A089 187 ATMOSPHERIC SCIENCE ASSOCIATES BEDFORD MASS F/G 15/6
SIMFIC: A SIMPLE, EFFICIENT FALLOUT PREDICTION MODEL.(U)
DEC 79 H G NORMENT DNA001-76-C-0010

UNCLASSIFIED DNA-5193F NL

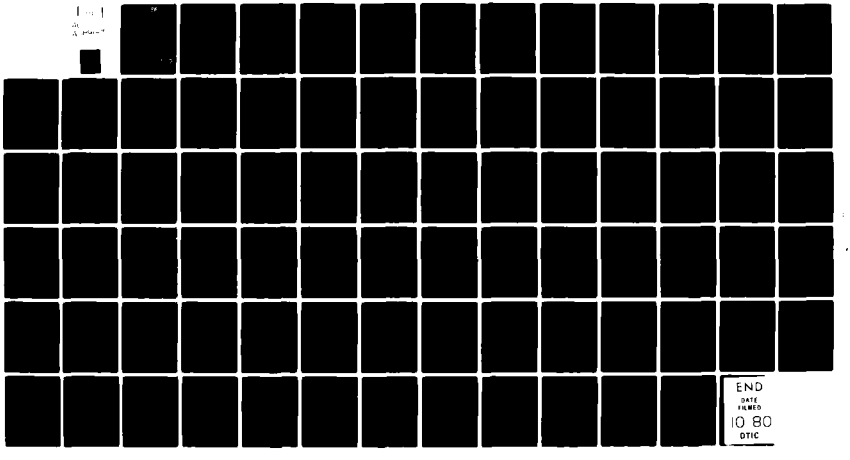

END
DATE FILMED
10 80
DTIC

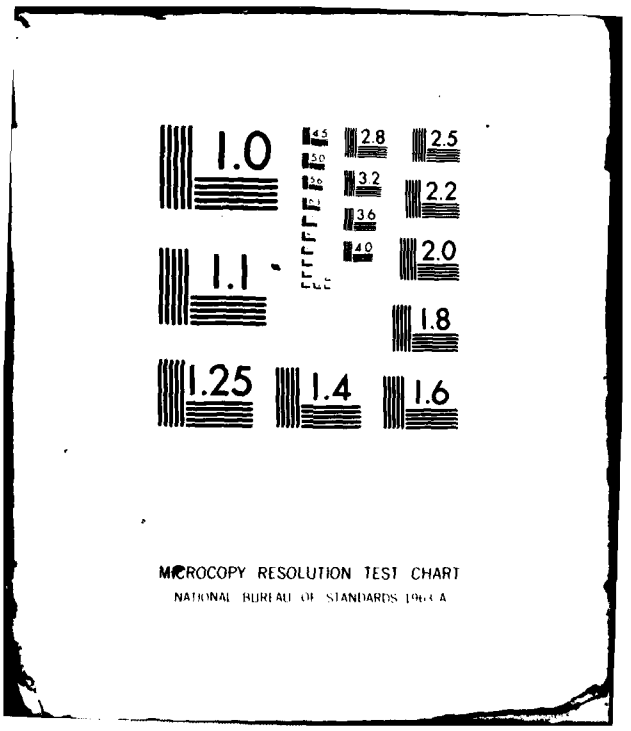
1.0
1.1
1.25
1.4
1.6
1.8
2.0
2.2
2.5
2.8
3.2
3.6
4.0
MICROCOPY RESOLUTION TEST CHART
NATIONAL BUREAU OF STANDARDS 1963 A

(12) LEVEL II

DNA 5193F

SIMFIC: A SIMPLE, EFFICIENT FALLOUT PREDICTION MODEL

Atmospheric Science Associates
P.O. Box 307
Bedford, Massachusetts 01730

31 December 1979

Final Report for Period 16 January 1979—31 December 1979

CONTRACT No. DNA 001-76-C-0010

APPROVED FOR PUBLIC RELEASE;
DISTRIBUTION UNLIMITED.

THIS WORK SPONSORED BY THE DEFENSE NUCLEAR AGENCY
UNDER RDT&E RMSS CODE B325079464 V99QAXNA00102 H2590D.

Prepared for
Director
DEFENSE NUCLEAR AGENCY
Washington, D. C. 20305

Destroy this report when it is no longer needed. Do not return to sender.

PLEASE NOTIFY THE DEFENSE NUCLEAR AGENCY, ATTN: TISI, WASHINGTON, D.C. 20305, IF YOUR ADDRESS IS INCORRECT, IF YOU WISH TO BE DELETED FROM THE DISTRIBUTION LIST, OR IF THE ADDRESSEE IS NO LONGER EMPLOYED BY YOUR ORGANIZATION.

17 A001 18 DNA, SBIE

UNCLASSIFIED

SECURITY CLASSIFICATION OF THIS PAGE (When Data Entered)

REPORT DOCUMENTATION PAGE

READ INSTRUCTIONS BEFORE COMPLETING FORM

1. REPORT NUMBER: DNA 5193F
2. GOVT ACCESSION NO.: AD-A089 187
3. RECIPIENT'S CATALOG NUMBER:

4. TITLE (and Subtitle): SIMFIC: A SIMPLE, EFFICIENT FALLOUT PREDICTION MODEL.
5. TYPE OF REPORT & PERIOD COVERED: Final Report, [redacted] 16 Jan [redacted]—31 Dec 79
6. PERFORMING ORG. REPORT NUMBER:

7. AUTHOR(s): Hillyer G. Norment
8. CONTRACT OR GRANT NUMBER(s): DNA 001-76-C-0010

9. PERFORMING ORGANIZATION NAME AND ADDRESS: Atmospheric Science Associates, P.O. Box 307, Bedford, Massachusetts 01730
10. PROGRAM ELEMENT, PROJECT, TASK AREA & WORK UNIT NUMBERS: Subtask V99QAXNA001-02

11. CONTROLLING OFFICE NAME AND ADDRESS: Director, Defense Nuclear Agency, Washington, D.C. 20305
12. REPORT DATE: 31 Dec [redacted]79
13. NUMBER OF PAGES: 82

14. MONITORING AGENCY NAME & ADDRESS (if different from Controlling Office): 5193F, AD-E300912
15. SECURITY CLASS (of this report): UNCLASSIFIED
15a. DECLASSIFICATION/DOWNGRADING SCHEDULE: 12 81

16. DISTRIBUTION STATEMENT (of this Report)

Approved for public release; distribution unlimited.

17. DISTRIBUTION STATEMENT (of the abstract entered in Block 20, if different from Report)

18. SUPPLEMENTARY NOTES

This work sponsored by the Defense Nuclear Agency under RDT&E RMSS Code B325079464 V99QAXNA00102 H2590D.

19. KEY WORDS (Continue on reverse side if necessary and identify by block number)

Nuclear Fallout	Fallout Prediction
Nuclear Weapons Effects	SIMFIC
Fallout Modeling	DELFIC

20. ABSTRACT (Continue on reverse side if necessary and identify by block number)

Details are given of the basis and mathematical structure of a fast, simple code, SIMFIC, for prediction of local fallout from surface and above surface nuclear weapon explosions. Verification results are presented for five test shot cases for which observed fallout patterns are available and which cover a yield range of 0.5 to 3380 KT. Prediction accuracy is as high as that obtained from the DELFIC code for these cases. Computing speed is on par with a code currently used for large-scale damage assessment studies. Other computing requirements are discussed briefly.

DD FORM 1 JAN 73 1473 EDITION OF 1 NOV 65 IS OBSOLETE

UNCLASSIFIED

SECURITY CLASSIFICATION OF THIS PAGE (When Data Entered)

392152

PREFACE

The author gratefully acknowledges the support and cooperation of Dr. David L. Auton of the Defense Nuclear Agency.

TABLE OF CONTENTS

LIST OF ILLUSTRATIONS

LIST OF TABLES

1. INTRODUCTION

A need has long been evident for a simple, fast numerical nuclear fallout prediction model with a capability approaching that of DELFIC,[1,2] but with greater accuracy and flexibility than WSEG-10.[3,4] Such a code could be used for operational work, such as damage assessment studies, and would be easily usable by those with less than total commitment to fallout research. A preliminary version of a model, SIMFIC (SIMplified Fallout Interpretive Code), that fills this need is described here. The physical and mathematical bases of the model are described in detail and validation results are presented. Computer requirements are discussed briefly. A complete description of the computer code is not included since at this time it is in a preliminary stage of development.

2. BASES OF THE SIMFIC MODEL

2.1 THE CENTRAL PROBLEM

With one notable exception, DELFIC, virtually all surface burst fallout prediction models are patterned after the RAND stabilized cloud model[5] which was developed about twenty-five years ago. This type of model is applicable to explosions with energy yields greater than about 1000 kiloton (KT) TNT equivalent. For such high yields emphasis is on the cloud cap which contains almost all of the airborne radioactive material at cloud stabilization time. On the other hand, for low yield explosions, a few tens KT or less, most of the close-in fallout is in the cloud stem. When a stabilized cloud model with an ill-defined or completely absent stem is used for such cases, as has all too frequently been done, prediction failure results as is clearly shown by recent studies.[6,7]

Experience with DELFIC shows that adequate treatments of atmospheric transport and radioactivity calculation are available. While problems remain regarding particle size and particle size-activity distribu tions, our most urgent concern is to define trajectories of particles, beginning at an early time in the fireball, through their rise along with the cloud, to gravity settlement and dispersion by the atmosphere. This must be done efficiently and rapidly, but with sufficient detail and fidelity to provide an accurate fallout prediction.

The key to solution of this problem lies in the well known fact that the altitude of a rising buoyant bubble is approximately proportional to the square root of its rise time. This has been observed, for example, by Norment and Woolf for nuclear clouds[8] and by Scorer for water tank experiments.[9] It was used by Anderson[10] in an earlier fallout model.

In SIMFIC the altitude-square root of time relationship is used to set up particle trajectory equations in the vertical. These are solved such as to develop equations from which the maximum altitude and the time it is reached can be determined for any particle. With this information along with ambient wind data, horizontal trajectory components are added such as to define the ground impact point for any particle taking into account wind advection throughout the entire period of its rise and settlement. This is done for a sufficient number of representative particles to adequately define the fallout pattern.

Details are presented in the remainder of this chapter.

2.2 VERTICAL TRAJECTORY EQUATIONS

In accord with the proportionality of cloud altitude with the square root of time, the altitudes of cloud (cap) base and top, z_B and z_T, at time t are given by linear interpolation on $\sqrt{t}$ between initial and final altitudes, $z_{B,i}$, $z_{T,i}$ and $z_{B,s}$, $z_{T,s}$, as

$$z_B = z_{B,i} + \frac{\sqrt{t} - \sqrt{t_i}}{\sqrt{t_s} - \sqrt{t_i}} (z_{B,s} - z_{B,i}) \qquad (2.2.1B)$$

$$z_T = z_{T,i} + \frac{\sqrt{t} - \sqrt{t_i}}{\sqrt{t_s} - \sqrt{t_i}} (z_{T,s} - z_{T,i}) \qquad (2.2.1T)$$

where the cloud rise is taken to begin at time t_i after detonation and end at time t_s. Differentiation of equations (2.2.1B and 2.2.1T) give the base and top velocities

$$u_B = \frac{z_{B,s} - z_{B,i}}{2\sqrt{t}(\sqrt{t_s} - \sqrt{t_i})} \qquad (2.2.2B)$$

$$u_T = \frac{z_{T,s} - z_{T,i}}{2\sqrt{t}(\sqrt{t_s} - \sqrt{t_i})} \qquad (2.2.2T)$$

Following the procedure used in DELFIC, which apparently follows Anderson,[10] we assume a linear variation of rise speed inside the cloud between z_B and z_T. Thus the vertical velocity of an in-cloud particle at altitude z with settling speed f is

$$\frac{dz}{dt} = u_B + (z - z_B)(u_T - u_B/(z_T - z_B) - f;\ z > z_B,\ t < t_s \qquad (2.2.3)$$

Also following DELFIC, we assume that upward drift velocity of air below the cloud decreases linearly with distance from the cloud base, which gives for the below-cloud particle velocity

$$\frac{dz}{dt} = zu_B/z_B - f;\ z \le z_B,\ t < t_s \ . \qquad (2.2.4)$$

At this point it is expedient to normalize the variables as follows:

$$\zeta = z/(z_{B,s} - z_{B,i}) \qquad (2.2.5)$$

$$\tau = \sqrt{t}/(\sqrt{t_s} - \sqrt{t_i}) \qquad (2.2.6)$$

$$v = d\zeta/d\tau = 2\tau u(\sqrt{t_s} - \sqrt{t_i})^2/(z_{B,s} - z_{B,i}), \qquad (2.2.7)$$

and a normalized, average settling speed (see sec. 2.5) is defined as

$$\hat{f} = < f > (\sqrt{t_s} - \sqrt{t_i})^2/(z_{B,s} - z_{B,i}) \quad . \tag{2.2.8}$$

In normalized form the equations above become

$$\zeta_B = \zeta_{B,i} + \tau - \tau_i \tag{2.2.1Bn}$$

$$\zeta_T = \zeta_{T,i} + (\tau - \tau_i)(\zeta_{T,s} - \zeta_{T,i}) \tag{2.2.1Tn}$$

$$v_B = 1 \tag{2.2.2Bn}$$

$$v_T = \zeta_{T,s} - \zeta_{T,i} \quad . \tag{2.2.2Tn}$$

For the in-cloud particle we have

$$v = 1 + (\zeta - \zeta_{B,i} - \tau + \tau_i)/(\tau - \tau_i + a) - 2\tau\hat{f};\ \zeta > \zeta_B, \tau < \tau_s \tag{2.2.3n}$$

where

$$a = (\zeta_{T,i} - \zeta_{B,i})/(\zeta_{T,s} - \zeta_{T,i} - 1) \quad , \tag{2.2.9}$$

and for the below-cloud particle we have

$$v = \zeta/(\tau - \tau_i + \zeta_{B,i}) - 2\tau\hat{f};\ \zeta \leq \zeta_B,\ \tau < \tau_s \quad . \tag{2.2.4n}$$

After the cloud stops rising we have

$$v = -2\tau\hat{f};\ \tau > \tau_s \quad . \tag{2.2.10}$$

Equations (2.2.3n), (2.2.4n) and (2.2.10) can be integrated to give the vertical trajectory equations:

In-cloud

$$\zeta - \zeta_i = (a + \zeta_i + \zeta_{B,i})(\tau - \tau_i)/a - 2\hat{f}(\tau - \tau_i + a)\left[\tau - \tau_i + (\tau_i - a)\ell n\left(\frac{\tau - \tau_i + a}{a}\right)\right]; \ \zeta > \zeta_B, \ \tau < \tau_o, \ \tau < \tau_s \quad (2.2.11)$$

Below-cloud

$$\zeta - \zeta_o = \zeta_o(\tau - \tau_o)/(\tau_o - \tau_i + \zeta_{B,i}) - 2\hat{f}(\tau - \tau_i + \zeta_{B,i})\left[\tau - \tau_o + (\tau_i - \zeta_{B,i})\ell n\left(\frac{\tau - \tau_i + \zeta_{B,i}}{\tau_o - \tau_i + \zeta_{B,i}}\right)\right]; \ \zeta \le \zeta_B, \ \tau_o < \tau < \tau_s \quad (2.2.12)$$

After completion of cloud rise

$$\zeta = \zeta_{\tau=\tau_s} - \hat{f}(\tau^2 - \tau_s^2); \ \tau > \tau_s \ . \quad (2.2.13)$$

Here τ_o and ζ_o are the time and altitude of separation of the particle from the cloud cap. Next we address the problem of the determination of τ_o and ζ_o.

2.3 TIME AND ALTITUDE OF PARTICLE SEPARATION FROM THE CLOUD

Fallout from the cloud cap occurs when $\zeta = \zeta_B$. By substituting eq. (2.2.1Bn) into the left side of eq. (2.2.11) and manipulating the result algebraically we arrive at

$$\tau_o - \tau_i + a + (\tau_i - a)\ell n(\tau_o - \tau_i + a) = (\zeta_i - \zeta_{B,i})/(2a\hat{f}) + (\tau_i - a)\ell n(a) + a \ . \quad (2.3.1)$$

Equations (2.2.3n), (2.2.4n) and (2.2.10) can be integrated to give the vertical trajectory equations:

In-cloud

$$\zeta - \zeta_i = (a + \zeta_i + \zeta_{B,i})(\tau - \tau_i)/a - 2\hat{f}(\tau - \tau_i + a)\left[\tau - \tau_i + (\tau_i - a)\ell n\left(\frac{\tau - \tau_i + a}{a}\right)\right]; \ \zeta > \zeta_B, \ \tau < \tau_o, \ \tau < \tau_s \quad (2.2.11)$$

Below-cloud

$$\zeta - \zeta_o = \zeta_o(\tau - \tau_o)/(\tau_o - \tau_i + \zeta_{B,i}) - 2\hat{f}(\tau - \tau_i + \zeta_{B,i})\left[\tau - \tau_o + (\tau_i - \zeta_{B,i})\ell n\left(\frac{\tau - \tau_i + \zeta_{B,i}}{\tau_o - \tau_i + \zeta_{B,i}}\right)\right] \ ; \ \zeta \le \zeta_B, \ \tau_o < \tau < \tau_s \quad (2.2.12)$$

After completion of cloud rise

$$\zeta = \zeta_{\tau=\tau_s} - \hat{f}(\tau^2 - \tau_s^2) \ ; \ \tau > \tau_s \ . \quad (2.2.13)$$

Here τ_o and ζ_o are the time and altitude of separation of the particle from the cloud cap. Next we address the problem of the determination of τ_o and ζ_o.

2.3 TIME AND ALTITUDE OF PARTICLE SEPARATION FROM THE CLOUD

Fallout from the cloud cap occurs when $\zeta = \zeta_B$. By substituting eq. (2.2.1Bn) into the left side of eq. (2.2.11) and manipulating the result algebraically we arrive at

$$\tau_o - \tau_i + a + (\tau_i - a)\ell n(\tau_o - \tau_i + a) = (\zeta_i - \zeta_{B,i})/(2a\hat{f}) + (\tau_i - a)\ell n(a) + a \ . \quad (2.3.1)$$

This has the form

$$\xi + b\ell n(\xi) = c \qquad (2.3.2)$$

which can be solved for ξ by Newton iteration. Then $\tau_o = \xi + \tau_i - a$, and ζ_o is found by substituting τ_o into eq. (2.2.1Bn).

2.4 MAXIMUM PARTICLE HEIGHT

The quantities actually used in the fallout prediction are the maximum altitude of the particle and the time this altitude is reached.

For in-cloud particles, set the left side of eq. (2.2.3n) to zero, solve for ζ_m, the maximum altitude, in terms of τ_m, the time at which ζ_m is reached,

$$\zeta_m = \zeta_{B,i} - a + 2\tau_m \hat{f}(\tau_m - \tau_i + a) \qquad (2.4.1)$$

and substitute this into eq. (2.2.11). After algebraic manipulation we arrive at an equation of the same form as eq. (2.3.2), but for which

$$\xi = \tau_m - \tau_i + a$$

$$b = (\tau_i - a)/2$$

$$c = (a + \zeta_i - \zeta_{B,i})/(4\hat{f}a) + b\ell n(a) + \tau_i/2 + a.$$

As with eq. (2.3.2) this is solved for ξ by Newton iteration, τ_m is recovered from ξ, and ζ_m is found by substitution of τ_m into eq. (2.4.1).

For below-cloud particles, set the left side of eq. (2.2.4n) to zero, solve for ζ_m in terms of τ_m,

$$\zeta_m = 2\tau_m \hat{f}(\tau_m - \tau_i + \zeta_{B,i}) \qquad (2.4.2)$$

substitute this into eq. (2.2.12), and after algebraic manipulation we again arrive at an equation of the form of eq. (2.3.2), but with

$$\xi = \tau_m - \tau_i + \zeta_{B,i}$$

$$b = (\tau_i - \zeta_{B,i})/2$$

$$c = \zeta_o/\left[4\hat{f}(\tau_o - \tau_i + \zeta_{B,i})\right] + \tau_o/2 + b\ell n(\tau_o - \tau_i + \zeta_{B,i}) - \tau_i + \zeta_{B,i}.$$

As before this is solved for ξ by Newton iteration, etc.

To select appropriate values for τ_m, ζ_m various possibilities must be examined. (Subscripts IC and BC denote in-cloud and below-cloud):

1. If $\tau_o > \tau_s$ and $\tau_m|_{IC} > \tau_s$, then set $\tau_m = \tau_s$ and calculate ζ_m by substitution of τ_s into eq. (2.2.11).

2. If $\tau_o > \tau_s$ and $\tau_m|_{IC} \leq \tau_s$, then use $(\tau_m, \zeta_m)_{IC}$.

3. If $\tau_o \leq \tau_s$ and $\tau_s \geq \tau_m|_{BC} > \tau_o$ and $\zeta_m|_{BC} > \zeta_m|_{IC}$ or $\tau_m|_{IC} > \tau_o$ use $(\tau_m, \zeta_m)_{BC}$.

4. If $\tau_o \leq \tau_s$ and $\tau_m|_{BC} > \tau_o$ and $\zeta_m|_{BC} > \zeta_m|_{IC}$ or $\tau_m|_{IC} > \tau_o$, but $\tau_m|_{BC} > \tau_s$ then set $\tau_m = \tau_s$ and compute ζ_m by substitution of τ_s into eq. (2.2.12).

To save computer time, z_m and t_m are computed only for particles at the base and top of the initial cloud for each particle size. For particles at intermediate initial positions, the following interpolation formula gives acceptable results

$$t_m = t_{m,B} + k^{0.85}\,(t_{m,T} - t_{m,B}) \qquad (2.4.3)$$

and

$$z_m = z_{m,B} + k^{0.85} (z_{m,T} - z_{m,B}) \qquad (2.4.4)$$

where

$$k = (z_i - z_{B,i})/(z_{T,i} - z_{B,i}) \ .$$

Computer plotted trajectories for particles initially at the initial cloud base and top for various particle sizes and weapon yields are presented in Appendix A.

2.5 ADVECTION AND SETTLING

A single vertical profile of wind vectors is input to the model. The altitudes at which the vectors are defined are used to stratify the atmosphere vertically into wind layers, in each of which a unique wind vector applies. Advection and settling of fallout particles is separated into two phases: 1. Rise of the particle to its maximum height z_m at time t_m, and 2. settlement of the particle from z_m to the ground. Thus, if $\vec{X}$ is the position vector, relative to ground zero, of a ground impacted fallout parcel we have

$$\vec{X} = \sum_{z=0}^{z_m} \vec{W}_z \Delta t \Big|_{rise} + \sum_{z=z_m}^{0} \vec{W}_z \Delta z/f \Big|_{settlement} \qquad (2.5.1)$$

where the summations are over the wind layers of depth Δz between the ground ($z = 0$) and the particle maximum height at z_m, Δt is the time spent in a wind layer, and $\vec{W}_z$ is the wind vector at height z.

During the rise phase, the particle altitude varies roughly as the square root of time. Therefore the time a particle spends in the ith wind layer, Δt_i, is approximately

$$\Delta t_i \simeq t_m \Delta(z^2)_i / z_m^2 \qquad (2.5.2)$$

where $\Delta(z^2)_i = z_{b,i+1}^2 - z_{b,i}^2$, and $z_{b,i}$ is the height of the base of the ith wind layer.

If we define an average settling speed between z_m and the ground, $< f >$, and substitute eq. (2.5.2) into (2.5.1) we obtain

$$\vec{X} = t_m z_m^{-2} \sum_{z=0}^{z_m} \vec{W}_z \Delta(z^2) + < f >^{-1} \sum_{z=0}^{z_m} \vec{W}_z \Delta z \quad . \qquad (2.5.3)$$

To avoid repetitive calculations of the sums in eq. (2.5.3), they are precalculated from the ground to each wind layer and stored. Then for each particle, the partial summands that account for transport to the base of the wind layer containing z_m are computed, and the balance of the transport to the ground is accounted for by adding to them the appropriate presummed quantities that are retrieved from storage.

The average particle settling speed is derived as follows. Best[11] has devised the simple equation

$$f = f_o e^{bz} \qquad (2.5.4)$$

for water drops, where f_o is settling speed at sea level, z is altitude (m) and

$$b = 2.90 \times 10^{-5}; \; 50 < \delta < 300 \; \mu m$$

$$b = 4.05 \times 10^{-5}; \; 300 \leq \delta < 6000 \; \mu m$$

where δ is water drop diameter. This equation also gives adequate results for fallout particles.

The average settling speed between altitudes z_1 and z_2 is determined by integration of eq. (2.5.4) to give

$$< f > = f_o\left(e^{bz_2} - e^{bz_1}\right) / \left[b(z_2 - z_1)\right] \quad . \tag{2.5.5}$$

In the SIMFIC code, a table of f_o values computed by the equations of Beard[12] and Davies[13] for fallout particles of density 2600 kg m^{-3} is stored for 75 particle sizes (see sec. 2.8).

2.6 CLOUD DEFINITION

Following DELFIC,[1] the initial cloud is defined at a time close to the fireball second temperature maximum

$$t_i = 2.07\ W^{0.19} \quad , s \ , \tag{2.6.1}$$

with radius

$$R_i = 108\ W^{0.33} \quad , m \ , \tag{2.6.2}$$

with base height

$$z_{B,i} = z_{GZ} + z_{HoB} + 90W^{1/3} \ , m \ , \tag{2.6.3}$$

and with top height

$$z_{T,i} = z_{B,i} + 1.32288\ R_i \ , m \quad . \tag{2.6.4}$$

Cloud stop and stabilization times are obtained by interpolation in $\log_{10}$ (W) from Table 1, which is taken from DELFIC simulations.

Stabilized cloud heights (m) are[14]

$$z_{B,s} = z_{GZ} + z_{HoB} + a\ W^b \qquad (2.6.5)$$

$$z_{T,s} = z_{GZ} + z_{HoB} + c\ W^d \qquad (2.6.6)$$

where

$a = 2228,\ b = 0.3463;\ W \leq 4.07$

$a = 2661,\ b = 0.2198;\ W > 4.07$

$c = 3597,\ d = 0.2553;\ W \leq 2.29$

$c = 3170,\ d = 0.4077;\ 2.29 < W \leq 19$

$c = 6474,\ d = 0.1650;\ W > 19$.

TABLE 1

CLOUD STOP AND STABILIZATION TIMES

Yield (KT)	Stop Time(s)	Stabilization Time(s)
10^{-3}	300	421
10^{-2}	300	421
10^{-1}	300	381
10^{0}	300	382
10^{1}	300	422
10^{2}	280	663
10^{3}	200	783
10^{4}	160	787
10^{5}	150	991

Stabilized cloud radius (m) is computed from

$$R_S = \exp(6.7553 + 0.7381Y + 0.060308Y^2) \qquad (2.6.7)$$

where $Y = \log_{10}(W)$.

In all cases above, W is yield in kilotons.

Any parcel of fallout that is inside the cloud cap at time t_m is given the stabilization radius R_S. (The difference between t_m and stabilization time is ignored.) For any size particle, the first separation from the cap is taken to occur at time t_i, and this wafer, which initially is at the initial cloud base, is given radius R_i. Its trajectory is followed to cloud stabilization, at which time its height, z_{min}, which may be below ground zero, is recorded. Parcels of fallout of this same particle size at height z are assigned stabilization radii

$$R = R_i + (z - z_{min})(R_S - R_i)/(z_{B,s} - z_{min});\ z_{min} \le z \le z_{B,s} \qquad (2.6.8)$$

At the initial time the cloud cap is partitioned into n subdivisions in the vertical for each particle size as illustrated in Fig. 1. n is either set to 5, which has been found to be adequate for all cases investigated to date, or

$$n = 10 + \log_{10}W\ , \qquad (2.6.9)$$

where W is yield in KT.

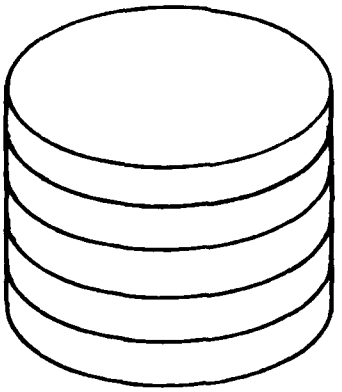

Figure 1. Subdivision of the initial cloud into five parcels, n = 5.

2.7 DISPERSION BY AMBIENT TURBULENCE

The same basic procedure is used here as in DELFIC.[1] Subsequent to t_m, each parcel of fallout is taken to have a Gaussian distribution in the horizontal with variance given by[15]

$$\sigma(t)^2 = \left[\sigma(t_m)^{2/3} + \frac{2}{3}\,\varepsilon^{1/3}\,(t - t_m)\right]^3;\ \sigma(t_m) \le \sigma(t) \le \sigma_\ell \qquad (2.7.1)$$

$$\sigma(t)^2 = \sigma_\ell^2 \left\{2(t - t_m)(\varepsilon/\sigma_\ell^2)^{1/3} + 3\left[\sigma(t_m)^2/\sigma_\ell^2\right]^{1/3} - 2\right\};\ \sigma(t) > \sigma_\ell \qquad (2.7.2)$$

where ε is turbulence energy density dissipation rate, σ_ℓ^2 is the parcel variance when its dispersion rate becomes constant, taken to be $10^9 m^2$, and $\sigma(t_m) = R/2$. (The difference between t_m and stabilization time is ignored.)

Using Wilkins'approximation for ε,[16] we define an average ε

$$\langle \varepsilon \rangle = 0.06/z_m$$

and an average settling time

$$< t > \; = \; z_m / < f >$$

where $< f >$ is average settling speed (sec. 2.5) and z_m is maximum parcel height above ground (sec. 2.4). Substituting these quantities into eqs. (2.7.1) and (2.7.2), we obtain at deposition time, t_d,

$$\sigma(t_d)^2 = \left[\sigma(t_m)^2 + 0.26099\, z_m^{2/3} / < f >\right]^3 ; \qquad (2.7.3)$$

$$z_m^{2/3} \leq 3.83155 < f > \left[10^3 - \sigma(t_m)^{2/3}\right]$$

$$\sigma(t_d)^2 = 7.8297 \times 10^5\, z_m^{2/3} / < f > + 3 \times 10^6 \sigma(t_m)^{2/3} - 2 \times 10^9 ; \qquad (2.7.4)$$

$$z_m^{2/3} > 3.83155 < f > \left[10^3 - \sigma(t_m)^{2/3}\right]$$

2.8 PARTICLE SIZE DISTRIBUTION, ACTIVITY CALCULATION AND MASS OF FALLOUT

A table of the 75 particle diameters larger than 50 μm from a set of 100 computed by DELFIC for a lognormal particle number distribution with median diameter 0.407 and geometric standard deviation 4.0 is stored. Corresponding to this table is stored a table of H + 1 hour exposure rate activity fractions calculated by DELFIC for a 0.5 KT fission yield for fission types[1] U238TN and P239HE and averaged.

A fallout prediction may be run using the complete table of 75 particle sizes, or it can be run using every other entry (38 particle sizes), every third entry (25 particle sizes), or every fourth entry (19 particle sizes).

K factors (Roentgens m^2 $hr^{-1}KT^{-1}$) for seven fission types also are stored and any one of these may be selected.

If the initial cloud is divided vertically into n fallout parcels for each particle size class (sec. 2.6), then the area integrated activity at a height of three feet above the ground from an impacted parcel of fallout in the ith particle size class is

$$Q = KW_F F_i \Phi / n \qquad (2.8.1)$$

where W_F is fission yield, F_i is the H + 1 hour exposure rate activity fraction in the ith particle size class and Φ is for exposure rate at time t (hours)

$$\Phi = t^{-1.26} ,$$

and for integrated exposure (dose) from time t_1 to t_2 (hours)

$$\Phi = (t_1^{-0.26} - t_2^{-0.26})/0.26 \quad .$$

Effect of height of burst above ground zero is accounted for approximately by multiplying the fission yield by the factor[17]

$$f_d = (0.45345)^{\lambda/65} \; ; \; \lambda > 0 \qquad (2.8.2)$$

where λ is scaled height of burst in units ft $KT^{-1/3}$. This factor is based on a curve of activity fraction down vs. scaled height of burst in Volume 5 of DASA 1251.

The DELFIC formulation of mass of fallout is used,[1]

$$m = 0.07704\, W^{3/3.4}(360 + \Lambda)(180 - \Lambda)^2; \; 0 \leq \Lambda \leq 180 \qquad (2.8.3)$$

where W is total yield in KT and Λ is scaled height of burst in units ft $KT^{-1/3.4}$.

SIMFIC does not have a subsurface burst capability.

2.9 DISTRIBUTION OF GROUNDED FALLOUT PARCELS

Following DELFIC[1] the top and base of each fallout parcel is transported separately to ground impaction. Then the impact point coordinates and variances of the two wafers are combined to form parameters for a bivariate Gaussian function which is used to distribute the parcel mass or activity over the impact plane.

If the total mass or area integrated activity in the parcel is Q, then the mass per unit area or activity contributed by this parcel at point x,y in the impact plane, $\omega(x,y)$, is

$$\omega(x,y) = \frac{Q}{2\pi\sigma_{\shortparallel}\sigma_{\perp}} \exp\left[-\frac{(X-X_p)^2}{2\sigma_{\shortparallel}^2} - \frac{(Y-Y_p)^2}{2\sigma_{\perp}^2}\right] \tag{2.9.1}$$

where

$$\begin{aligned} X &= x\cos\alpha + y\sin\alpha \\ Y &= y\cos\alpha - x\sin\alpha \end{aligned} \tag{2.9.2}$$

and X_p and Y_p are defined similarly. The parcel central coordinates, x_p, y_p, standard deviations, $\sigma_{\shortparallel}$, $\sigma_{\perp}$, and orientation angle α are determined from the coordinates and standard deviations of the impacted parcel top and base (subscripts t and b indicate top and base respectively) according to (see Fig. 2)

$$\begin{aligned} x_p &= (x_t + x_b)/2 \\ y_p &= (y_t + y_b)/2 \\ r &= \sqrt{(x_t - x_b)^2 + (y_t - t_b)^2} \end{aligned} \tag{2.9.3}$$

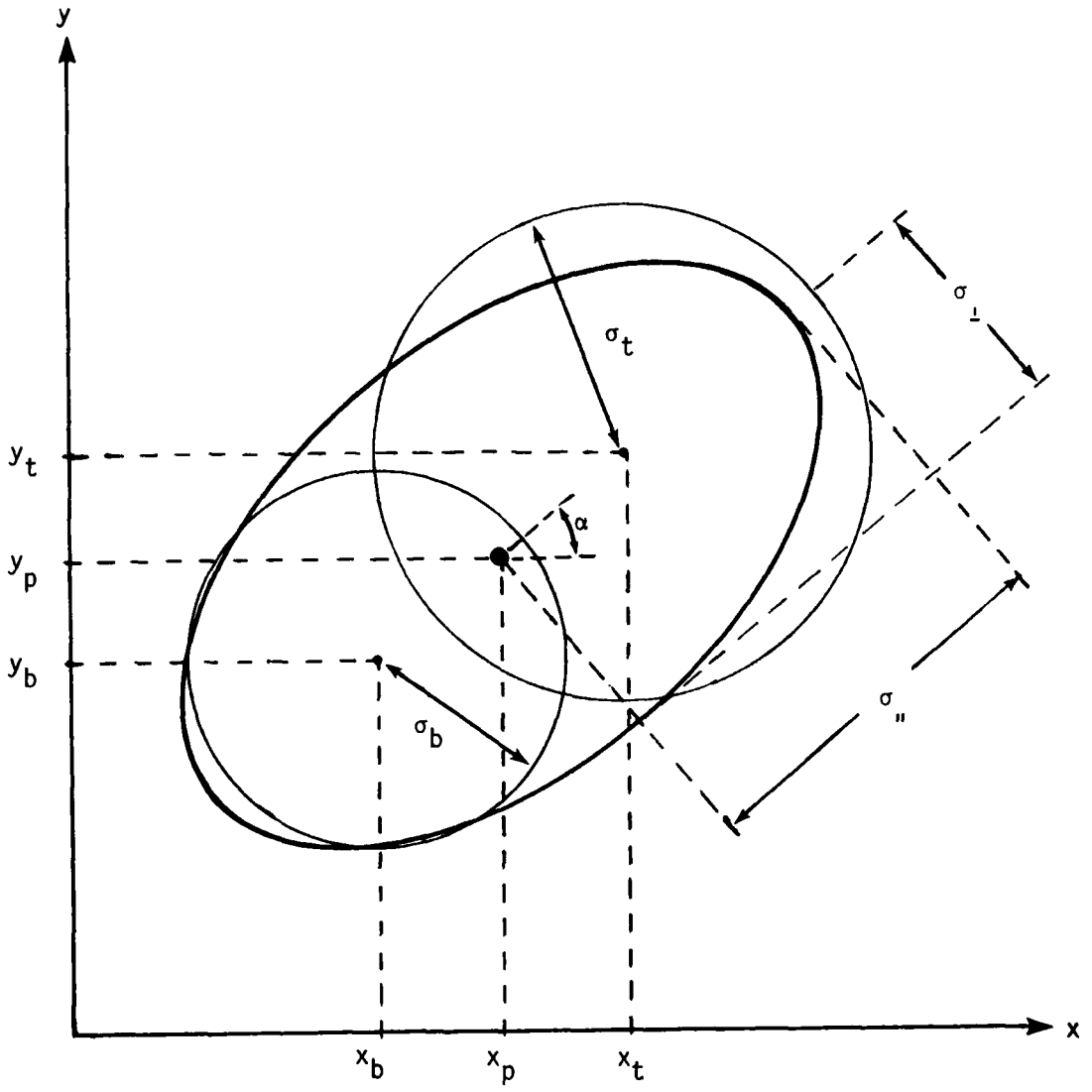

Figure 2. Synthesis of a deposit increment standard deviation ellipse from the impact points and standard deviations of the parcel top and base wafers.

$$\sigma_{\parallel}^2 = (\sigma_t + \sigma_b + r)^2/4$$

$$\sigma_{\perp}^2 = \sigma_t \sigma_b \qquad (2.9.4)$$

$$\cos\alpha = |x_t - x_b|/r$$

$$\sin\alpha = (x_t - x_b)(y_t - y_b)/(r|x_t - x_b|) \qquad (2.9.5)$$

To save time in accumulating contributions from parcels at map points, a table of 101 exponential function values, spanning the range of values expected for the type of map requested, is precomputed and stored. The exponential argument values of eq. (2.9.1) are computed as indicated, and then an approximate exponential function value is obtained directly from the table.

2.10 FALLOUT MAP PREPARATION

Any or all of the fifteen unique types of fallout maps described in Table 2 may be computed. Precisely the same procedure is used by SIMFIC as is used in DELFIC for map preparation.[1]

The user may specify map boundaries and grid increments or he may let the code supply these quantities. This is done by the code by considering wind direction, wind shear and explosion yield, and is included for use in an exploratory run to obtain a first-look at a fallout map.

TABLE 2

MAP REQUEST OPTIONS

Map Option Code	Description
1	Count of fallout deposit increments that contribute to each map ordinate.
2	Exposure rate normalized* to H + 1 hour (Roentgen hr^{-1}).
3	Exposure rate at time H + T1 hours, accounting for time of arrival of fallout. (Roentgen hr^{-1})
4	H + 1 hour normalized* exposure rate resulting from particles in diameter range T1 to T2 micrometers. (Roentgen hr^{-1})
5,9	Integrated exposure from H + T1 hours to infinity, accounting for time of arrival of fallout. (Roentgen)
6,10	Integrated exposure from H + T1 to H + T2 hours, accounting for time of arrival of fallout. (Roentgen)
7	Integrated exposure from H + T1 to H + T2 hours assuming all fallout has arrived by H + T1 hours. (Roentgen)
8	Integrated exposure from H + T1 hours to infinity assuming all fallout has arrived by H + T1 hours. (Roentgen)
11	Mass of fallout per unit area (kg m^{-3}).
12	Mass of fallout per unit area deposited from H + T1 to H + T2 hours (kg m^{-3}).
13	Mass of fallout per unit area deposited by particles in diameter range T1 to T2 micrometers. (kg m^{-3})
15	Time of onset of fallout. (s)
16	Time of cession of fallout. (s)
17	Diameter of smallest particle deposited. (μm)
18	Diameter of largest particle deposited. (μm)

*A "normalized" calculation is one in which it is assumed that all fallout is deposited by H + t regardless of actual deposition time.

3. COMPUTATION REQUIREMENTS

SIMFIC is a FORTRAN code presently operational on the CDC 6600 computer. Including extensive glossaries and comments, the code uses 1545 statement cards, which is about 3/4 of a box of cards. It uses less than 16,000 central memory storage words and no peripheral storage.

To obtain a benchmark computing time, the five predictions discussed in the next section were done in one run using five vertical cloud subdivisions (sec. 2.6) and nineteen particle sizes (sec. 2.8). Computing time was 10.5 seconds. The same five predictions were done in one run using the SEER code.[18] Twenty-five particle sizes were used and the code set the number of vertical cloud subdivisions ($n = 3 + \ell nW$); identical maps were produced in terms of boundaries, grid increments and numbers of points. Computing time was 7.4 seconds. Thus, SIMFIC is almost as fast as SEER, but produces much superior predictions.[6,7] (It also uses about one-third as much central processor storage as SEER.) For damage assessment work, where many predictions are required for fixed explosion yield, substantial savings of computing time could be realized without sacrifice of prediction accuracy and with only modest increase in central processor storage usage.

Data requirements of the code are minimal: yields (total and fission), height of burst above ground zero, ground zero height above sea level, fission type (optional), data for a single wind profile, map type code and quantities T1 and T2 if required (Table 2), map boundaries and grid intervals (optional*), and some simple control information.

*The code has a capability to set map boundaries and grid intervals based on wind direction, wind shear and yield.

4. VALIDATION

4.1 DISCUSSION

Predictions by SIMFIC and DELFIC are compared with observed H + 1 hour normalized* exposure rate maps for the five test shots described in Table 3. DELFIC predictions were executed as discussed in reference 7, using the data listed there. SIMFIC predictions were similarly executed using H hour winds only, with five cloud subdivisions (sec. 2.6) and nineteen particle sizes (sec. 2.8). Observed fallout patterns were taken from DASA 1251.

Three methods of comparison of fallout patterns are used:

1. Visual comparison of contour maps.
2. Comparison of contour areas, and hotline lengths and azimuths.**
3. The Rowland-Thompson Figure-of-Merit (FM).[19] (Appendix B)

These are roughly in order of importance.

Statistical data are in Table 4 and the contour plots are on pp. 30 through 44. The contours were drawn by a 30-inch Calcomp plotter, and members of each observed-predicted set are to the same scale.

TABLE 3

TEST SHOT DATA

Shot	Total Yield (KT)	Fission Yield (KT)	HOB (m)	Altitude of GZ (m)	Site
Johnie Boy	0.5	0.5	-0.584	1570.6	NTS+
Jangle-S	1.2	1.2	1.067	1284.7	NTS
Small Boy	low	-	3.048	938.2	NTS
Koon	150.	-	4.145	0.0	Bikini
Zuni	3380.	-	2.743	0.0	Bikini

+Nevada Test Site

*A "normalized" exposure rate map is constructed on the assumption that all local fallout is down at the specified time, regardless of its actual deposition time.

**Hotline length is defined as the furthest distance from ground zero on a contour, and hotline azimuth is the angle, measured clockwise from north, to the point of furthest distance from ground zero on a contour.

TABLE 4

COMPARISON OF OBSERVED AND PREDICTED FALLOUT PATTERN STATISTICS
Observed/DELFIC/SIMFIC

Test Shot	FM DELFIC SIMFIC	Contour (Roentgen hr^{-1})	Area(km^2)	Hotline Length(km)	Azimuth(deg)
Johnie Boy	0.182	1000	0.278/0.029/0.018	1.38/0.32/0.32	359/ 0/ 0
	0.152	100	0.539/0.774/0.781	2.73/2.58/2.69	345/344/344
		50	1.271/1.787/1.828	4.10/4.13/5.14	343/343/344
			58(42)/61(44)*	28(3)/34(13)*	
Jangle-S	0.483	500	0.117/0.144/0.156	0.69/1.00/1.60	342/353/351
	0.437	300	0.386/0.316/0.435	1.50/1.23/2.23	346/354/351
		100	1.437/2.242/1.278	3.74/5.87/3.40	1/355/352
		35	3.114/5.077/4.093	5.06/7.68/9.37	6/355/ 6
			40(45)/22(18)	43(42)/69(48)	
Small Boy	0.308	1000	0.216/0.047/0.144	1.00/0.25/0.60	71/ 66/ 80
	0.533	500	0.528/0.135/0.375	1.62/0.56/1.15	73/ 80/ 75
		200	0.942/0.564/1.031	2.22/1.69/2.17	72/ 73/ 71
		100	3.75/1.10/2.26	5.66/3.72/4.02	72/ 74/ 68
		50	9.03/4.38/7.59	8.10/6.47/8.17	75/ 72/ 66
			63(59)/25(24)	44(36)/20(15)	
Koon	0.287	500	32.0/26.0/44.0	10.2/12.5/14.9	18/ 0/ 0
	0.325	250	122/87.3/116	17.3/24.2/24.1	15/ 4/ 0
		100	550/261/374	41.0/39.5/41.6	17/ 3/ 1
			33(40)/25(18)	22(22)/29(20)	
Zuni	0.105	150	474/2239/2854	98/78/77	12/337/354
	0.189	100	2761/3619/4566	125/96/97	17/337/356
		50	6187/6660/9365	138/121/142	27/338/355
		30	10950/9913/15190	177/153/180	33/340/359
			105(16)/164(52)	17(16)/12(9)	

*Mean absolute percent errors: DELFIC/SIMFIC. The values in parentheses are calculated without including the data for the highest activity level contours. See footnote next page.

Prediction accuracy is seen to be good, particularly for the low yield shots. Overall mean absolute percent errors* for contour area and hotline length are:

	Contour Area	Hotline Length
DELFIC	61(42)	32(26)
SIMFIC	59(31)	32(21)

The quantities in parentheses are computed with the data for the highest activity level contours excluded. The highest level contours are particularly difficult to predict, usually being in the region affected by throwout and induced activity in and around the crater. SIMFIC and DELFIC do not address this portion of the activity field since fallout is a negligible contributor to casualties there. SIMFIC prediction accuracy is insensitive to numbers above five of vertical cloud subdivisions. Increasing the number of particle size classes smooths the patterns and eliminates the multiple contour closures in the Jangle-S prediction, but appears not to warrant the increased cost in computing time.

For these cases SIMFIC is shown to be at least equal to DELFIC in prediction accuracy. It is important to emphasize that this level of competency in SIMFIC has been achieved without a posteriori adjustment or calibration of any aspect of the model so as to improve agreement with any observed fallout pattern.

The three low yield shots were executed at the Nevada Test Site, and their fallout patterns were measured over land. For this reason, observed patterns for these shots, though not highly accurate, may be considered to

*For n observed-predicted data pairs, mean absolute percent error is

$$\frac{100}{n} \sum_{i=1}^{n} |x_{obs,i} - x_{pred,i}| / x_{obs,i} \quad .$$

be superior to the patterns of the high yield shots which were executed on Bikini Atoll in the South Pacific. Not only are the fallout fields of the high yield shots very large, which adds to measurement problems, but most of the fallout from these shots fell into water. Even so, most of the Koon pattern area was covered by an array of fallout collection stations, so this pattern is probably reasonably accurate. Zuni, on the other hand, is a special case. The fallout pattern used here is exclusively downwind of the atoll and was determined by an oceanographic survey method that was known to be inaccurate. The close-in pattern in the region of the atoll is available, but contains no closed contours so could not be used here; thus the high-activity portion of the observed pattern for this shot is ignored, and this alone must account for a substantial portion of the disagreement between observation and prediction for this shot, particularly with regard to contour areas and contour overlap (Table 4). In addition, we have the following problem.

Predictions for these high yield shots are expected to be inferior to those for these low yield shots. This is because both of the high yield shots were detonated over coral soil, and in the case of Zuni, a large but uncertain amount of sea water was lifted by the cloud. The particle size distribution used for these predictions is typical of fallout produced from the siliceous soil found at the Nevada Test Site. We have not succeeded in developing a distribution appropriate for coral and coral-sea water mixtures.

More details concerning the prediction calculations and test shot characteristics are in reference 7.

4.2 OBSERVED AND PREDICTED FALLOUT PATTERNS

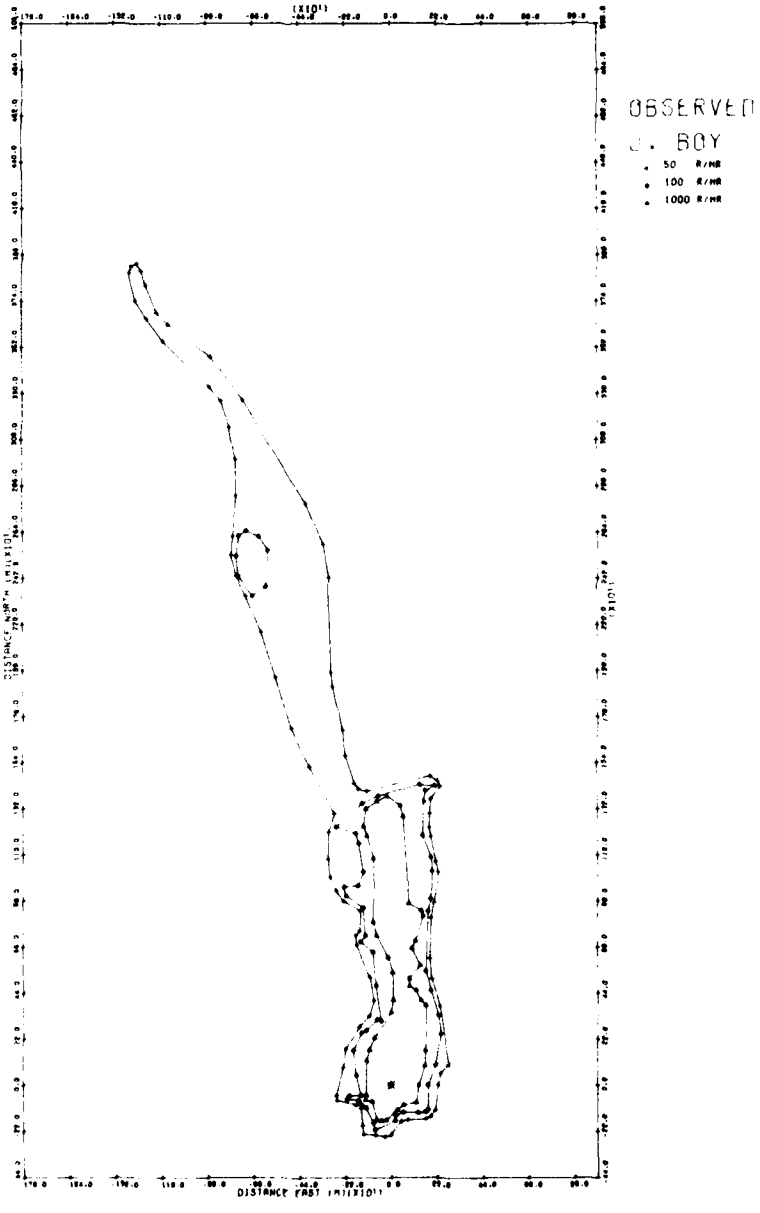
OBSERVED
BOY
50 R/HR
100 R/HR
1000 R/HR

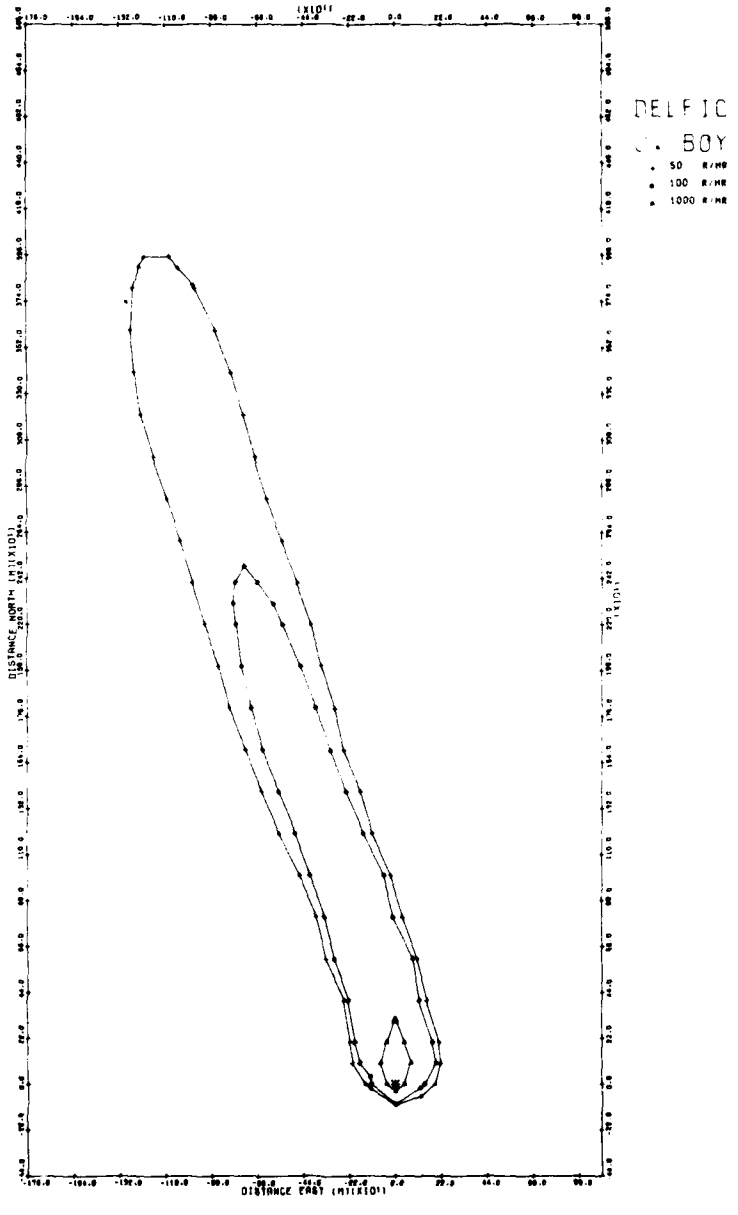
DISTANCE NORTH (MILES)
DISTANCE EAST (MILES)
DELFIC
BOY
50 R/HR
100 R/HR
1000 R/HR

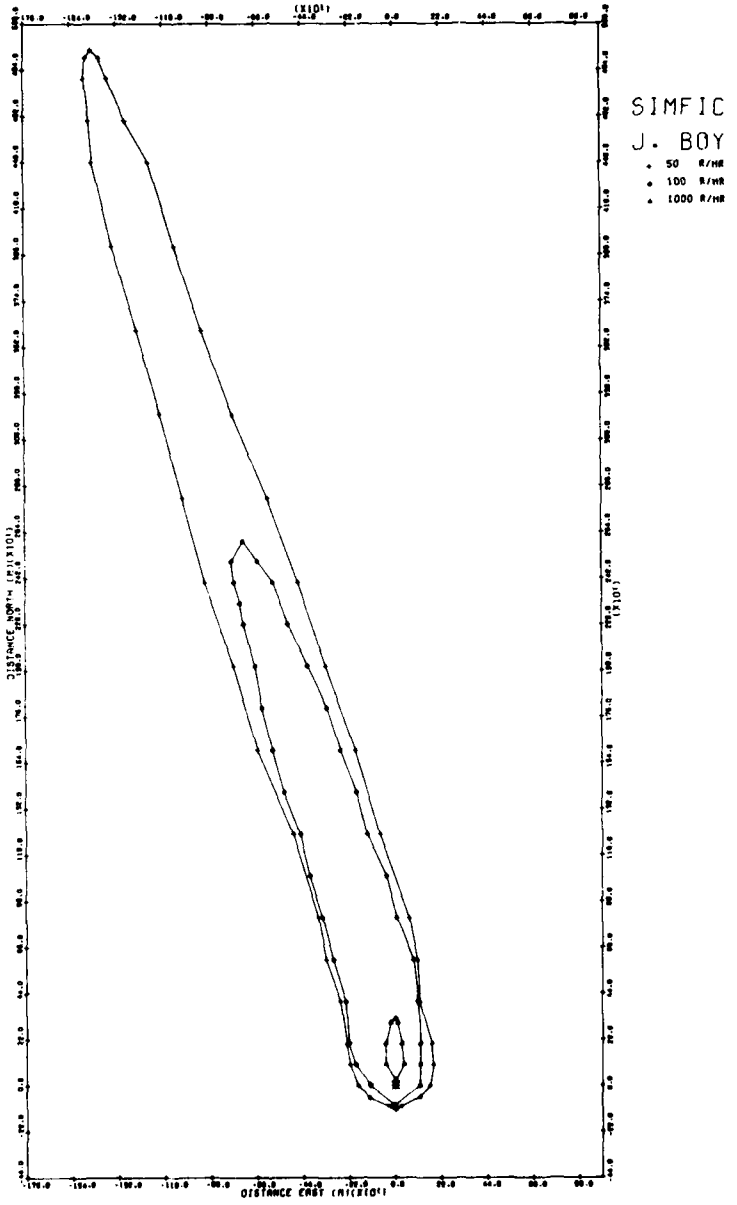
SIMFIC
J. BOY
50 R/HR
100 R/HR
1000 R/HR
DISTANCE EAST (X10¹)

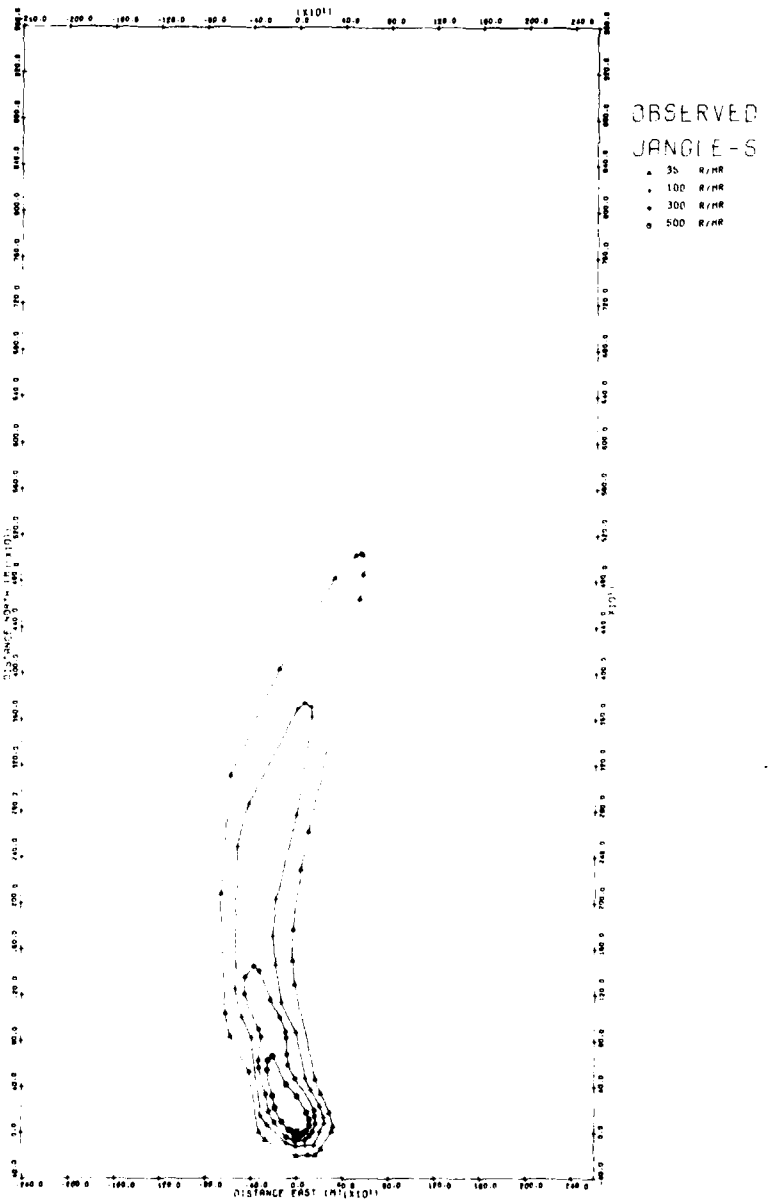
OBSERVED
JANGLE-S
35 R/HR
100 R/HR
300 R/HR
500 R/HR
DISTANCE EAST (M)(X10¹)

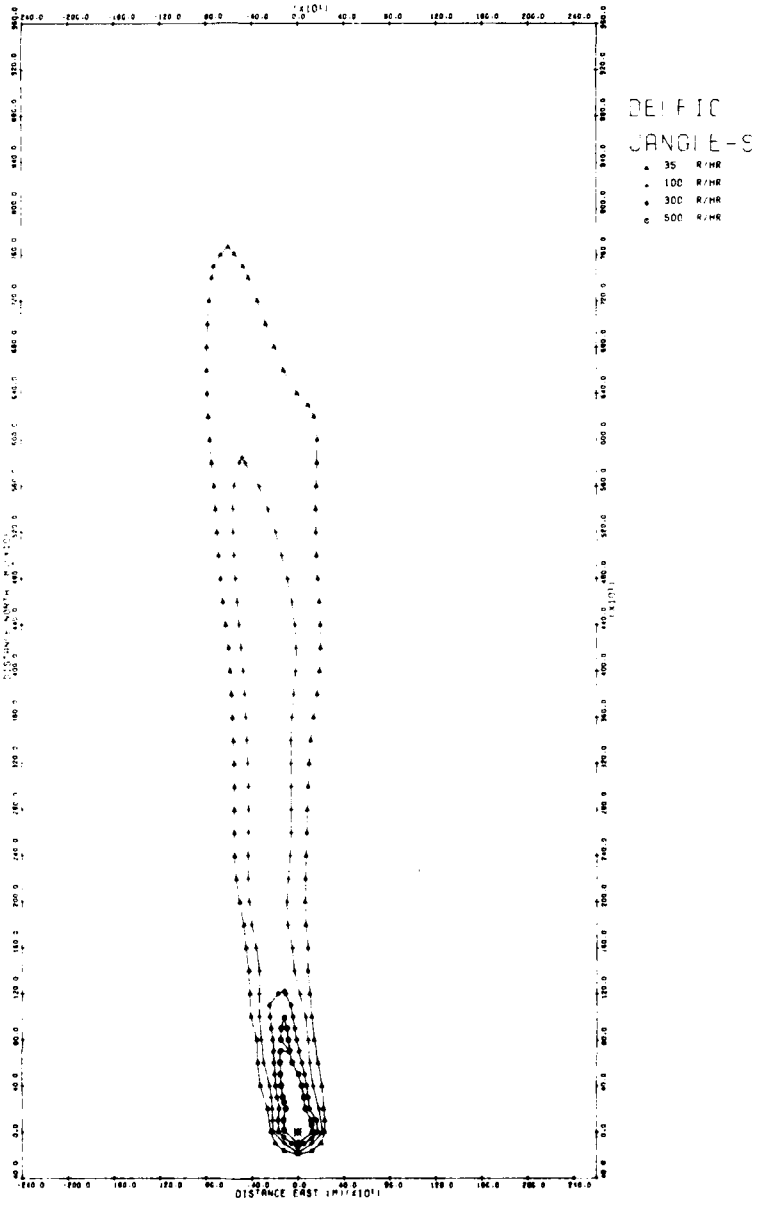
DISTANCE EAST
DELPIC
JANGLE-S
35 R/HR
100 R/HR
300 R/HR
500 R/HR

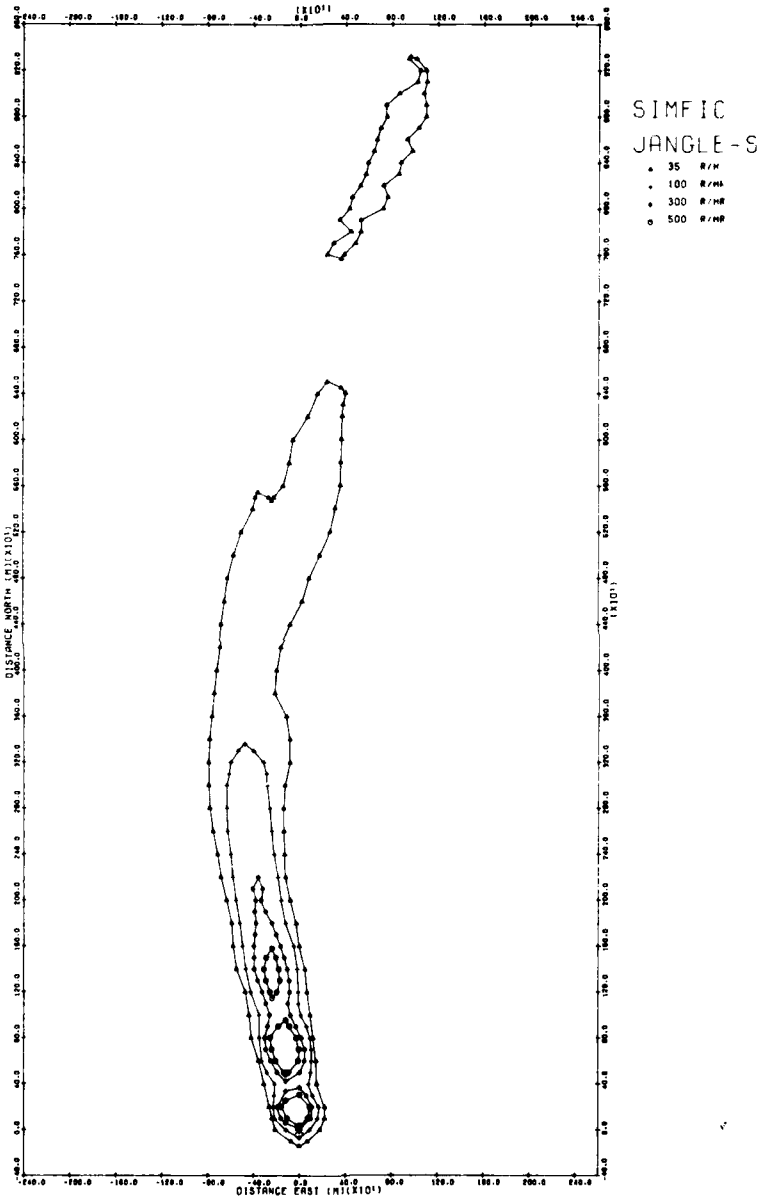
SIMFIC
JANGLE-S
35 R/H
100 R/HR
300 R/HR
500 R/HR
DISTANCE NORTH (MI)(X10)
DISTANCE EAST (MI)(X10)

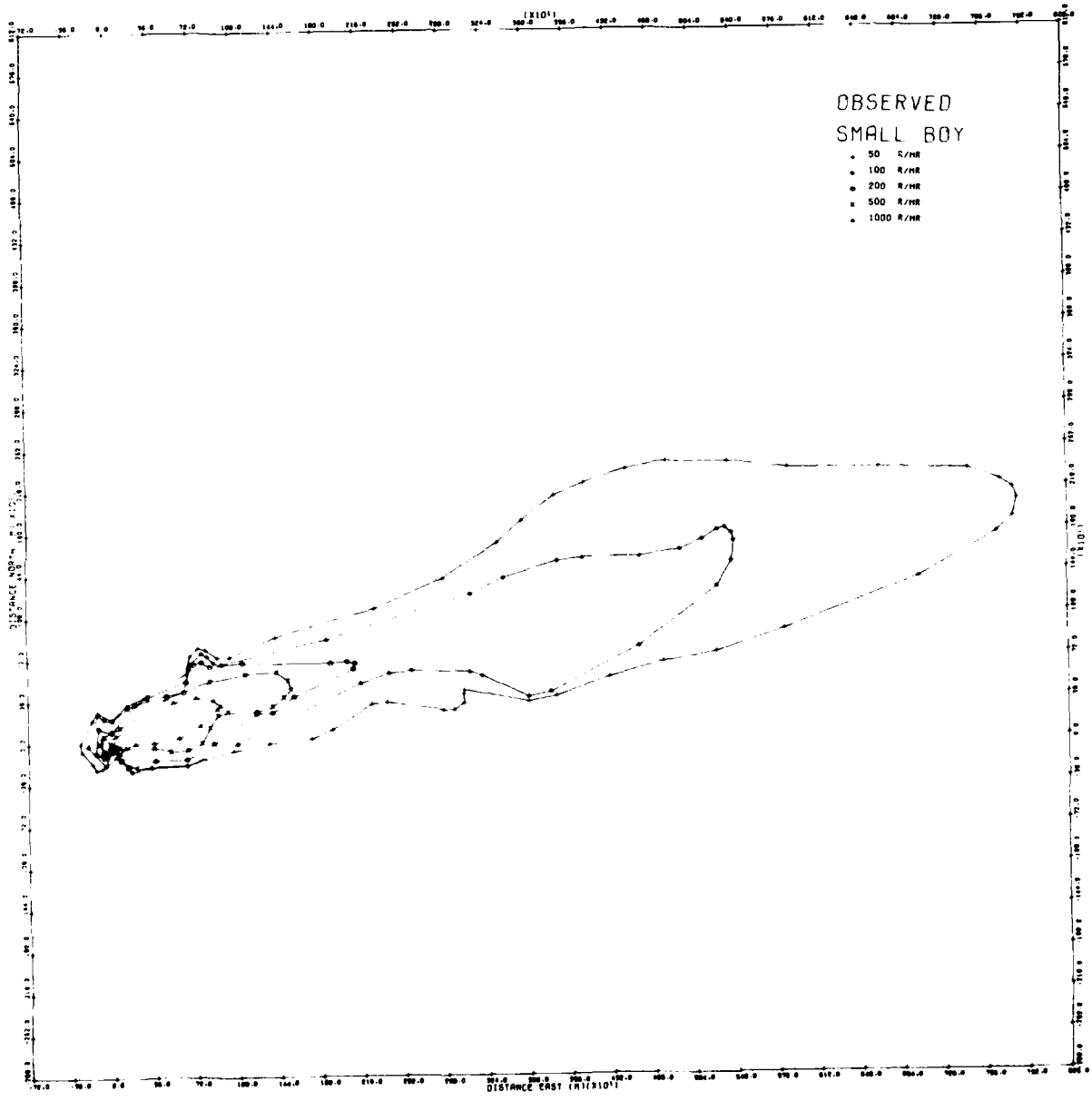
OBSERVED
SMALL BOY
50 R/HR
100 R/HR
200 R/HR
500 R/HR
1000 R/HR
DISTANCE EAST (R)(X10¹)

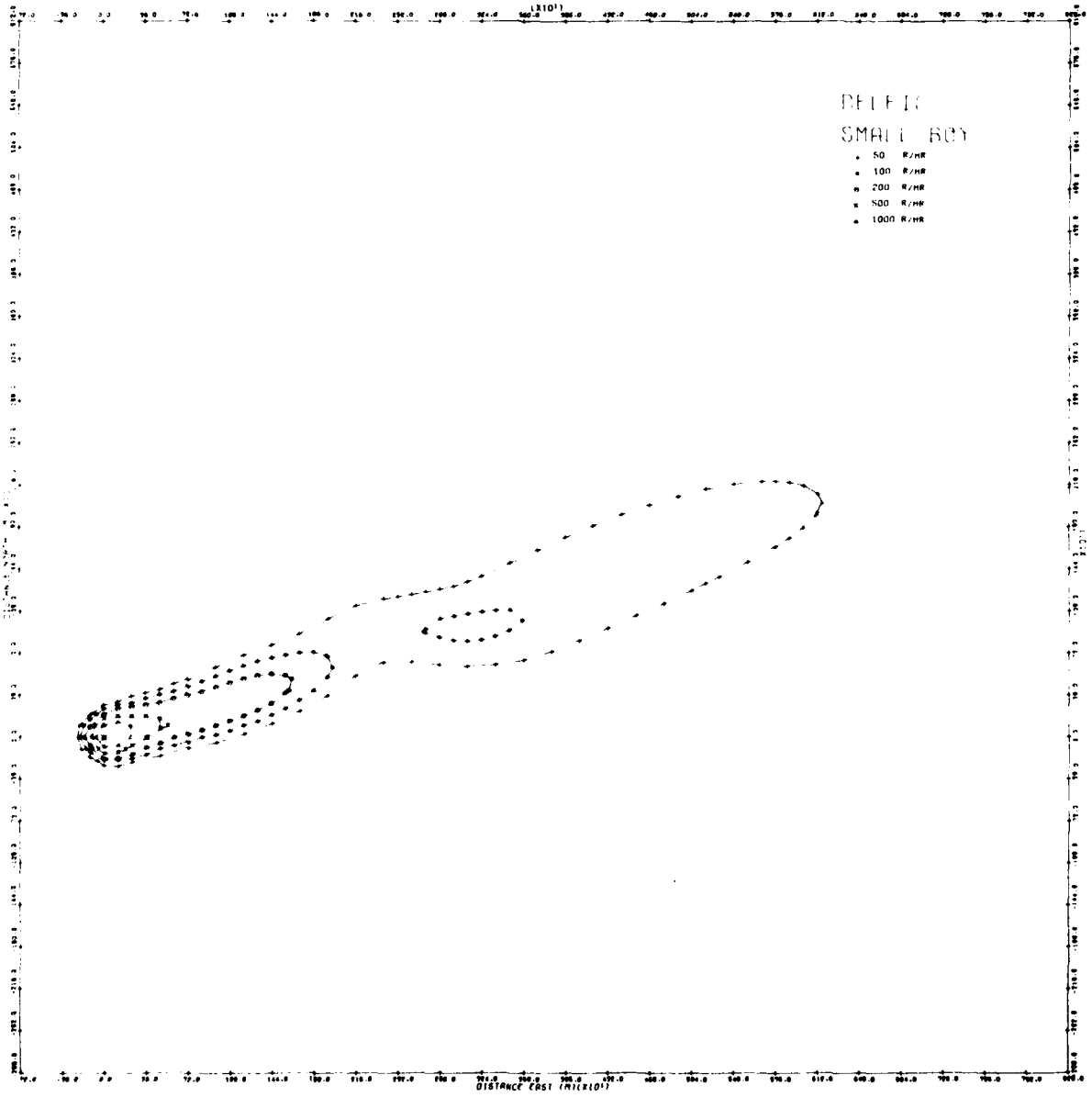
DELETE
SMALL BOY
50 R/HR
100 R/HR
200 R/HR
500 R/HR
1000 R/HR
DISTANCE EAST (NM X10¹)

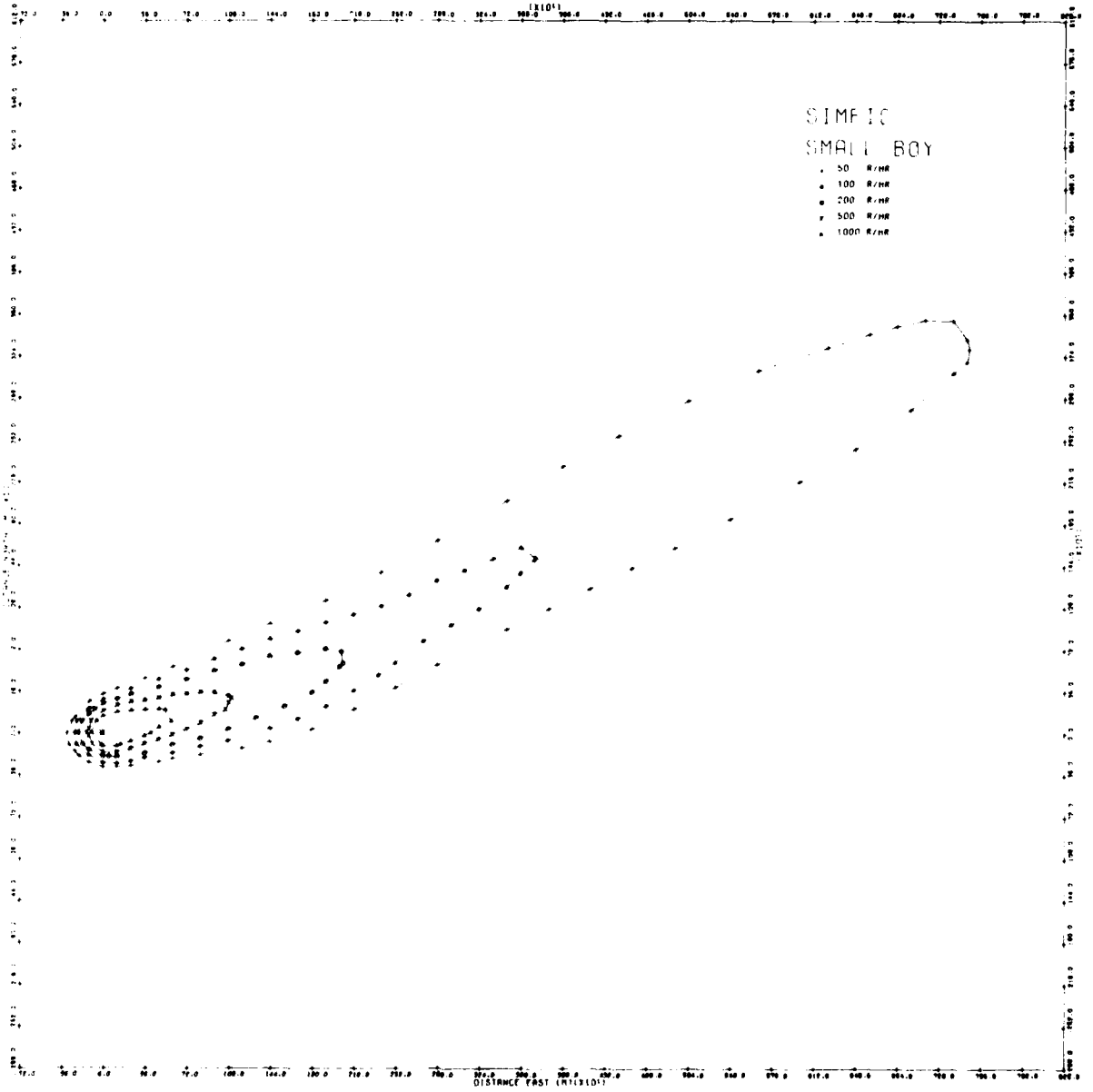
SIMPLE
SMALL BOY
50 R/HR
100 R/HR
200 R/HR
500 R/HR
1000 R/HR
DISTANCE EAST (FEET X10¹)

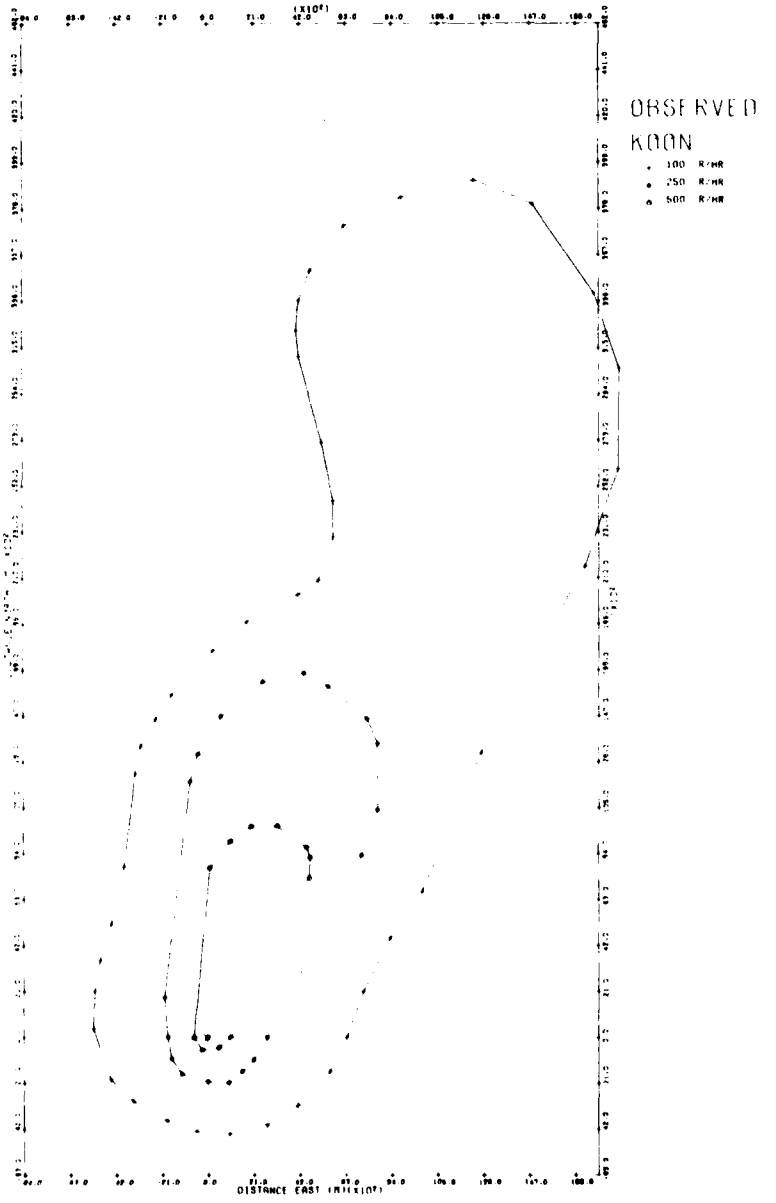
OBSERVED
KOON
100 R/HR
250 R/HR
500 R/HR
DISTANCE EAST (NTIES)

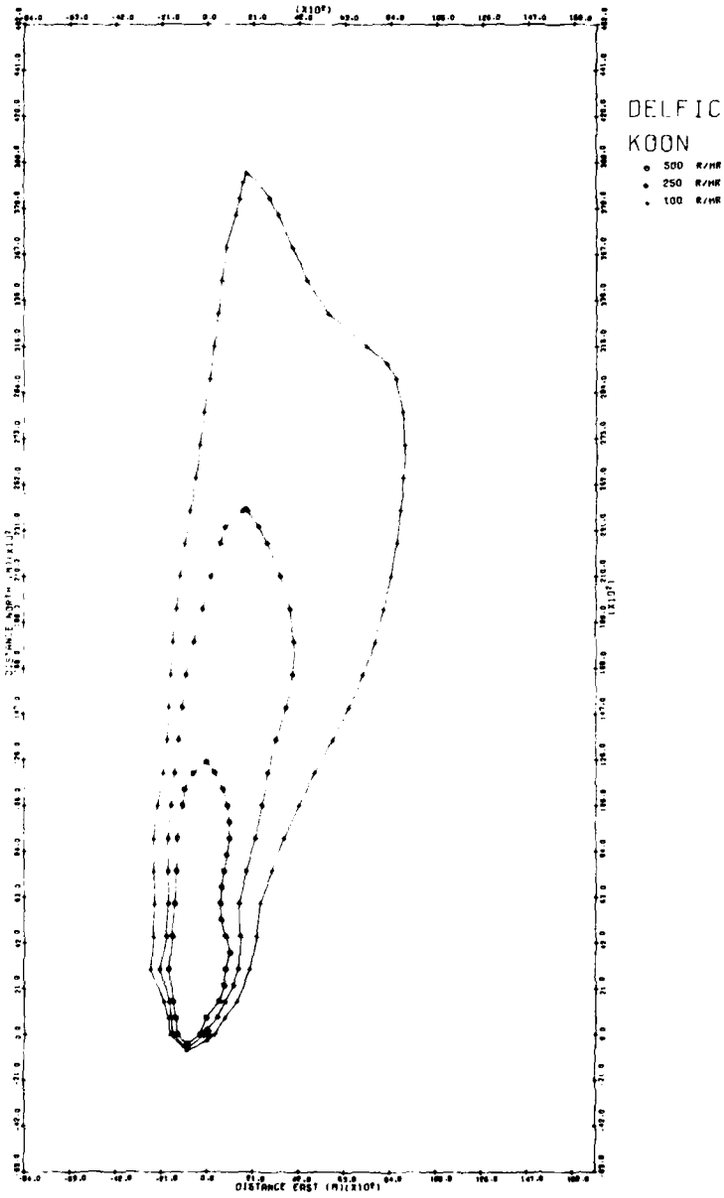
DELFIC
KOON
500 R/HR
250 R/HR
100 R/HR
DISTANCE EAST (M)(X10⁶)

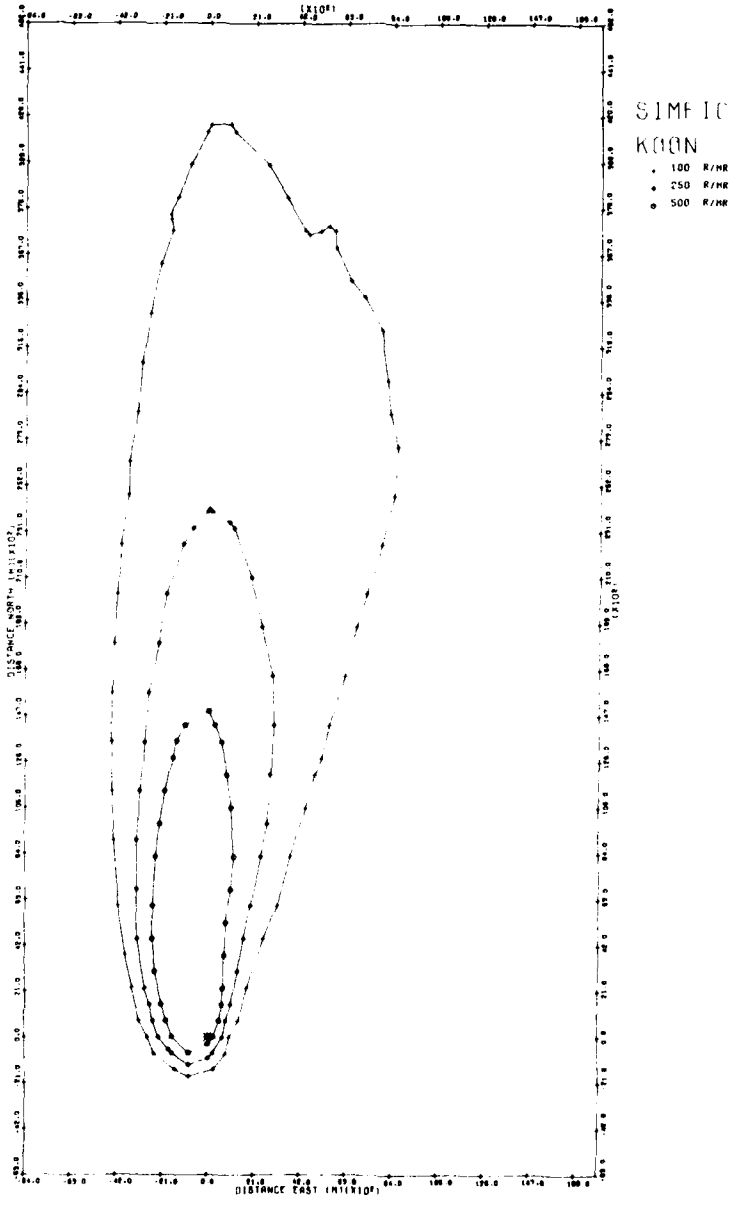
SIMFIC
KOON
100 R/HR
250 R/HR
500 R/HR
DISTANCE EAST (METERS)

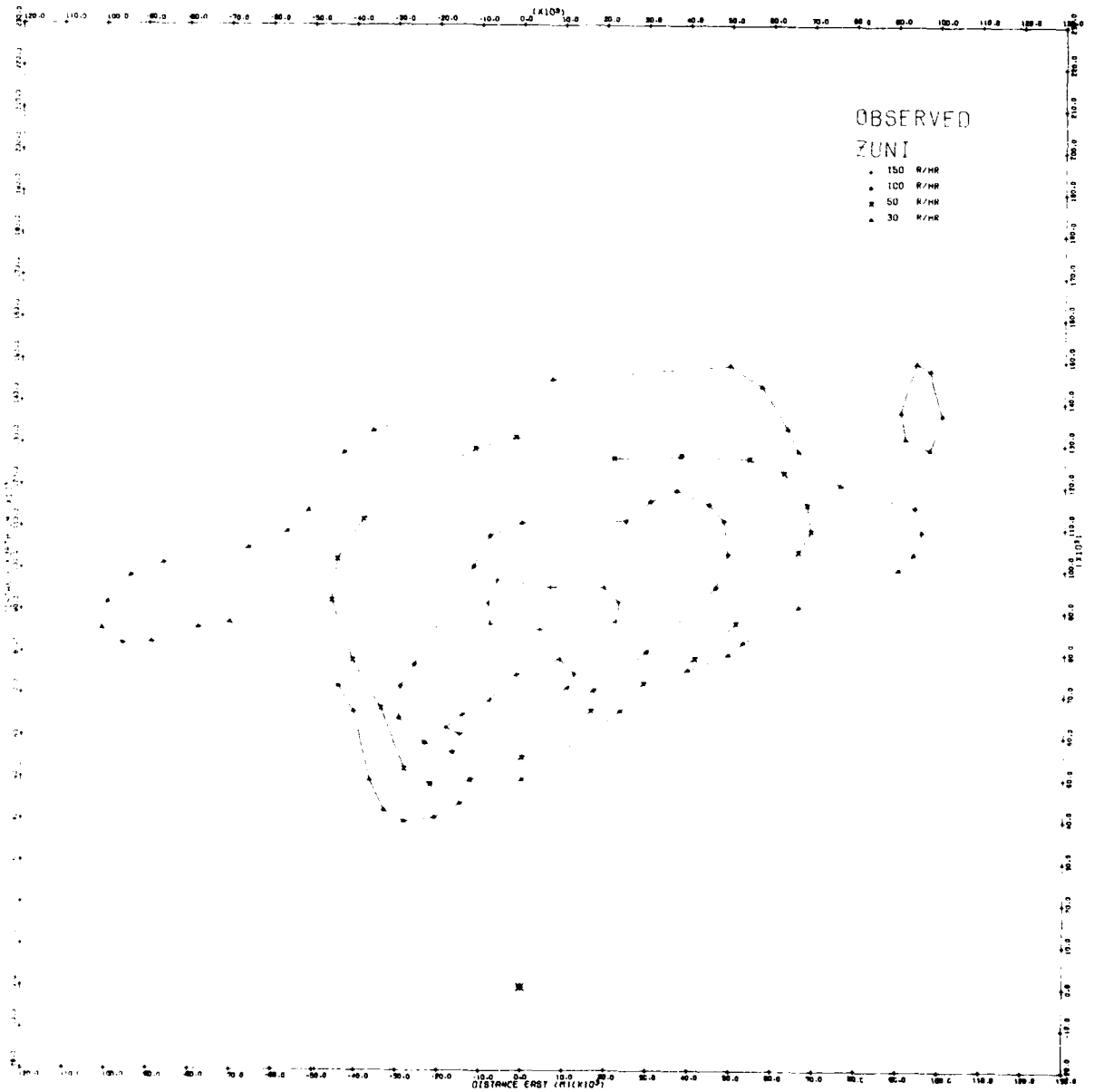
OBSERVED
ZUNI
150 R/HR
100 R/HR
50 R/HR
30 R/HR
DISTANCE EAST (MI)(X10³)

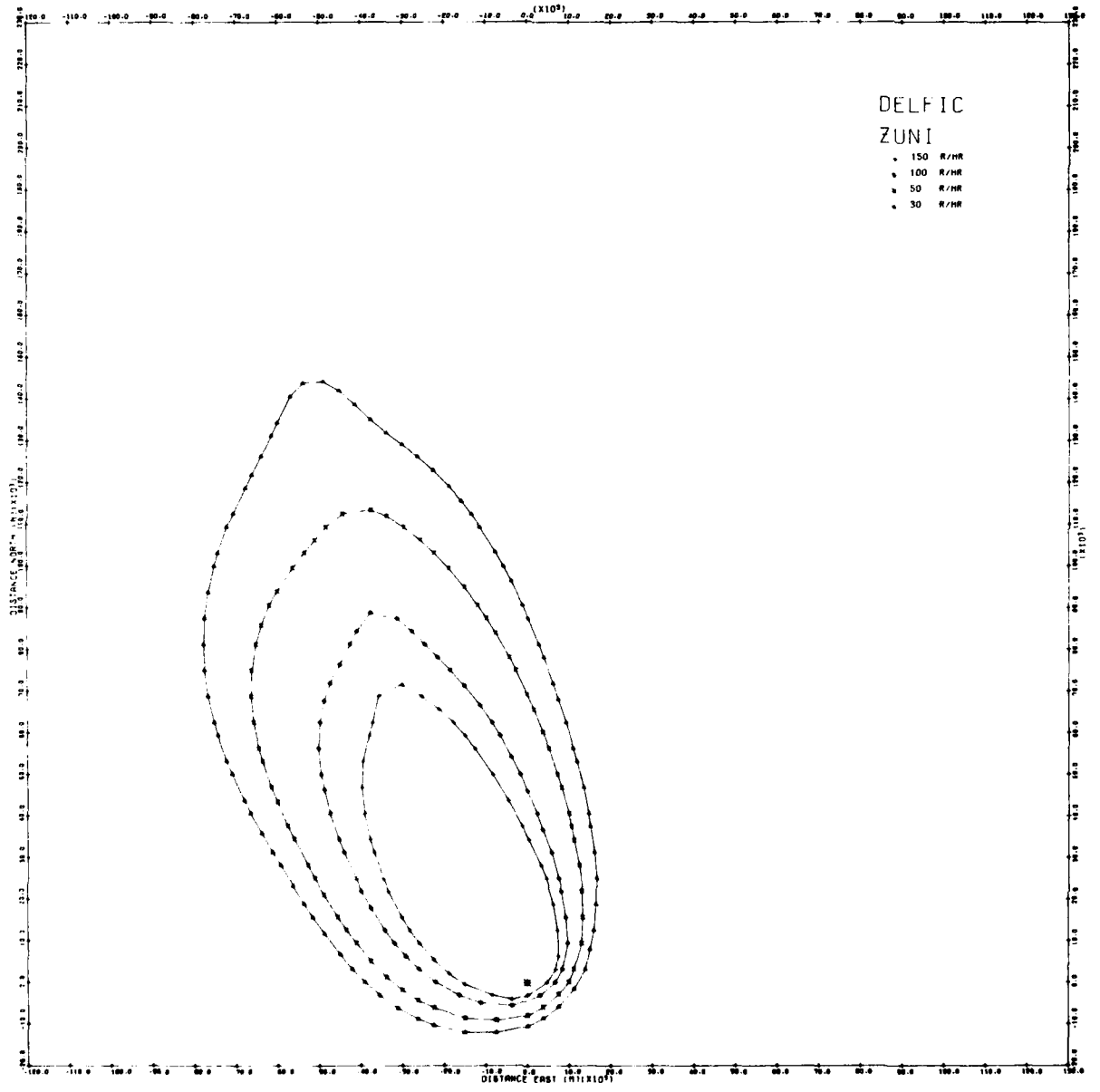
DELFIC
ZUNI
150 R/HR
100 R/HR
50 R/HR
30 R/HR
DISTANCE EAST (MI)(X10²)

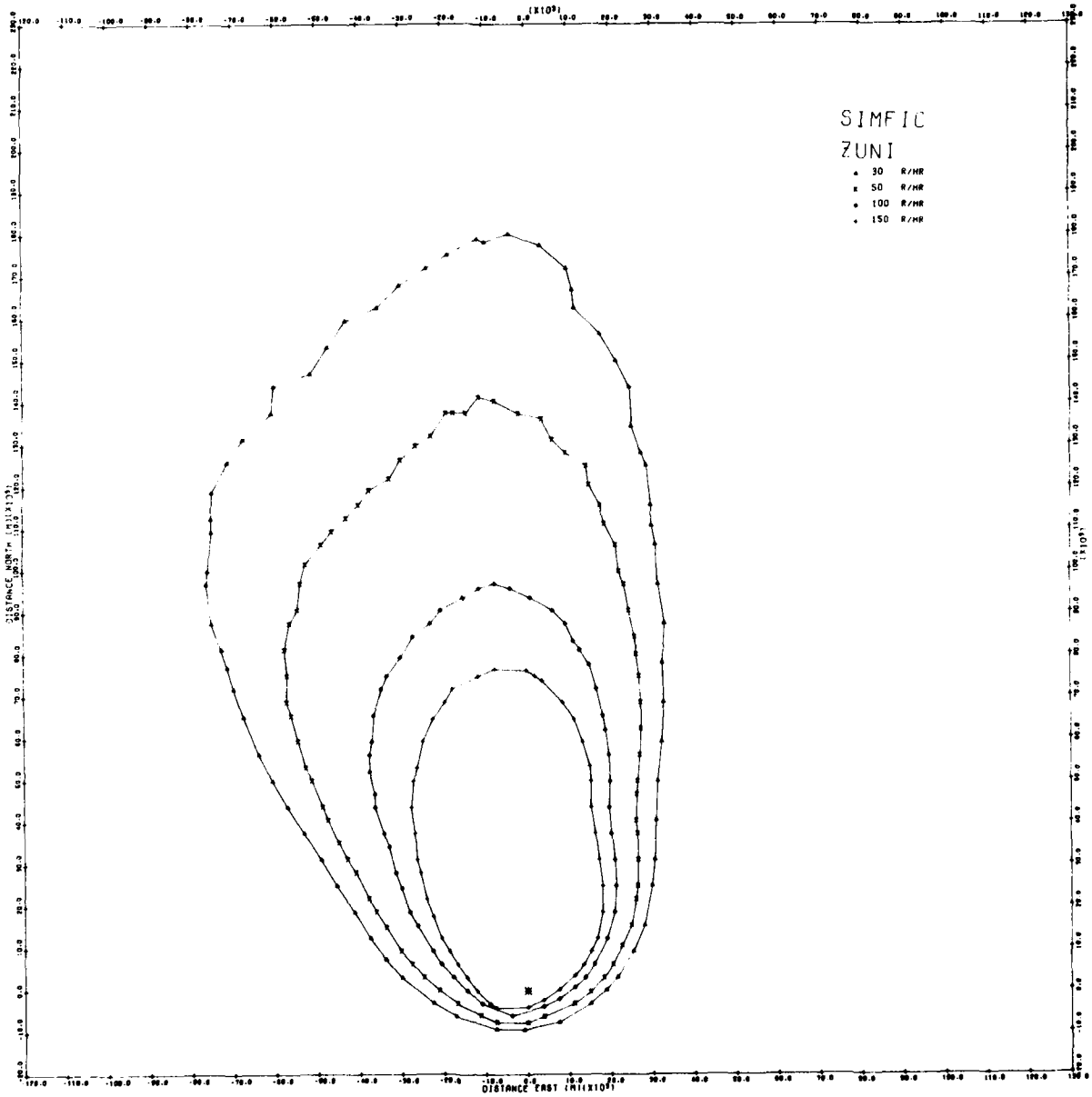
SIMFIC
ZUNI
30 R/HR
50 R/HR
100 R/HR
150 R/HR
DISTANCE EAST (MI)(X10³)

REFERENCES

1. H. G. Norment, "DELFIC: Department of Defense Fallout Prediction System. Volume I - Fundamentals," Atmospheric Science Associates, DNA 5159-1 (26 October 1979).

2. H. G. Norment, "DELFIC: Department of Defense Fallout Prediction System. Volume II - User's Manual," Atmospheric Science Associates, DNA 5159-2 (26 October 1979).

3. G. E. Pugh and R. J. Galiano, "An Analytical Model for Close-In Operational-Type Studies," Weapons Systems Evaluation Group, WSEG RM No. 10 (15 October 1959). AD 261 752.

4. R. B. Mason, "Description of Mathematics for the Single Integrated Damage Analysis Capability (SIDAC)," National Military Command System Support Center, NMCSSC TM 15-73 (1 July 1973). AD 913 164L.

5. W. W. Kellogg, R. R. Rapp and S. M. Greenfield, "Close-In Fallout," J. Meteor. 14, 1 (1957).

6. H. G. Norment, "Analysis and Comparison of Fallout Prediction Models," Atmospheric Science Associates, unpublished.

7. H. G. Norment, "Evaluation of Three Fallout Prediction Models: DELFIC, SEER and WSEG-10," Atmospheric Science Associates, DNA 5285F (16 June 1978).

8. H. G. Norment and W. Woolf, "Studies of Nuclear Cloud Rise and Growth," Technical Operations, Inc., unpublished.

9. R. S. Scorer, "Experiments on Convection of Isolated Masses of Buoyant Fluid," J. Fluid Mech. 2, 583 (1957).

10. A. D. Anderson, "A Theory for Close-In Fallout from Land-Surface Nuclear Bursts," J. Meteor. 18, 431 (1961).

11. A. C. Best, "Empirical Formulae for the Terminal Velocity of Water Drops Falling Through the Atmosphere," Quart. J. Roy. Meteor. Soc. 76, 302 (1950.

12. K. V. Beard, "Terminal Velocity and Shape of Cloud and Precipitation Drops Aloft," J. Atm. Sci. 33, 851 (1976).

REFERENCES, continued

13. C. N. Davies, "Definitive Equations for the Fluid Resistance of Spheres," Proc. Phys. Soc. (London) 57, 259 (1945).

14. E. F. Wilsey and C. Crisco, "An Improved Method to Predict Nuclear Cloud Heights," Ballistics Research Laboratory, unpublished.

15. J. J. Walton, "Scale Dependent Diffusion," J. Appl. Meteor. 12, 547 (1973).

16. E. M. Wilkins, "Decay Rates for Turbulent Energy Throughout the Atmosphere," J. Atm. Sci. 20, 473 (1963).

17. R. L. Showers, "Improvements to the PROFET Fallout Prediction Program," Ballistics Research Laboratories, BRL-MR-2095 (February 1971). AD-883 280.

18. H. Lee, P. W. Wong and S. L. Brown, "SEER II: A New Damage Assessment Fallout Model," Stanford Research Institute, DNA 3008F (May 1972). AD-754 144.

19. R. H. Rowland and J. H. Thompson, "A Method for Comparing Fallout Patterns," DASIAC, G.E. - Tempo, DNA 2919F (April 1972).

APPENDIX A

PARTICLE TRAJECTORIES

Computer drawn trajectories in the vertical computed by the methods of secs. 2.1 - 2.4 are presented for various particle sizes and weapon yields. All particles initially are at the initial cloud base or top. Heights and times are normalized according to eqs. (2.2.5) and (2.2.6). Yields are in KT and particle diameters in μm. Horizontal and vertical lines are drawn across the graphs to intersect at points of separation from the cloud cap and maximum height.

INITIALLY AT CLOUD BASE

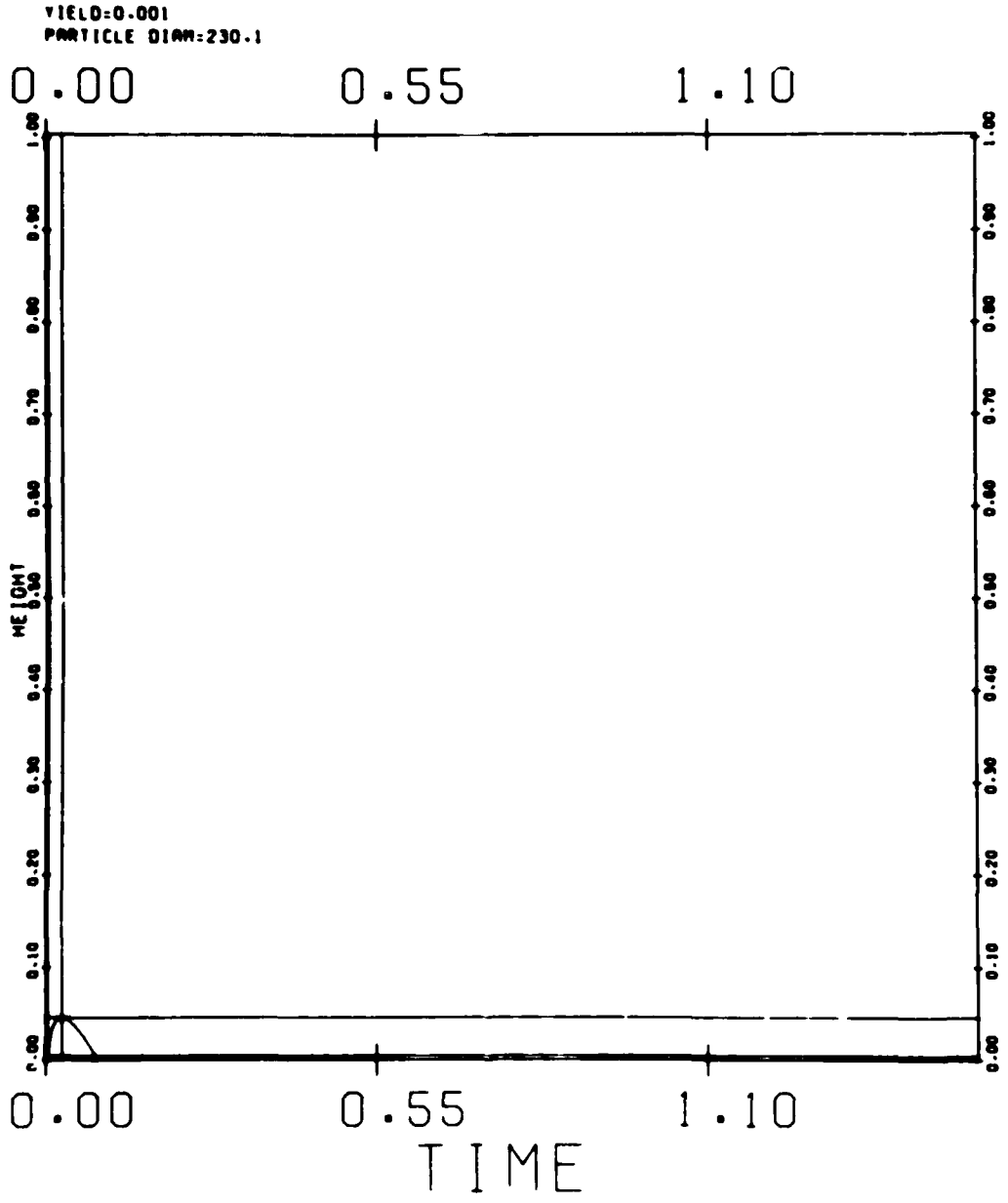

INITIALLY AT CLOUD TOP

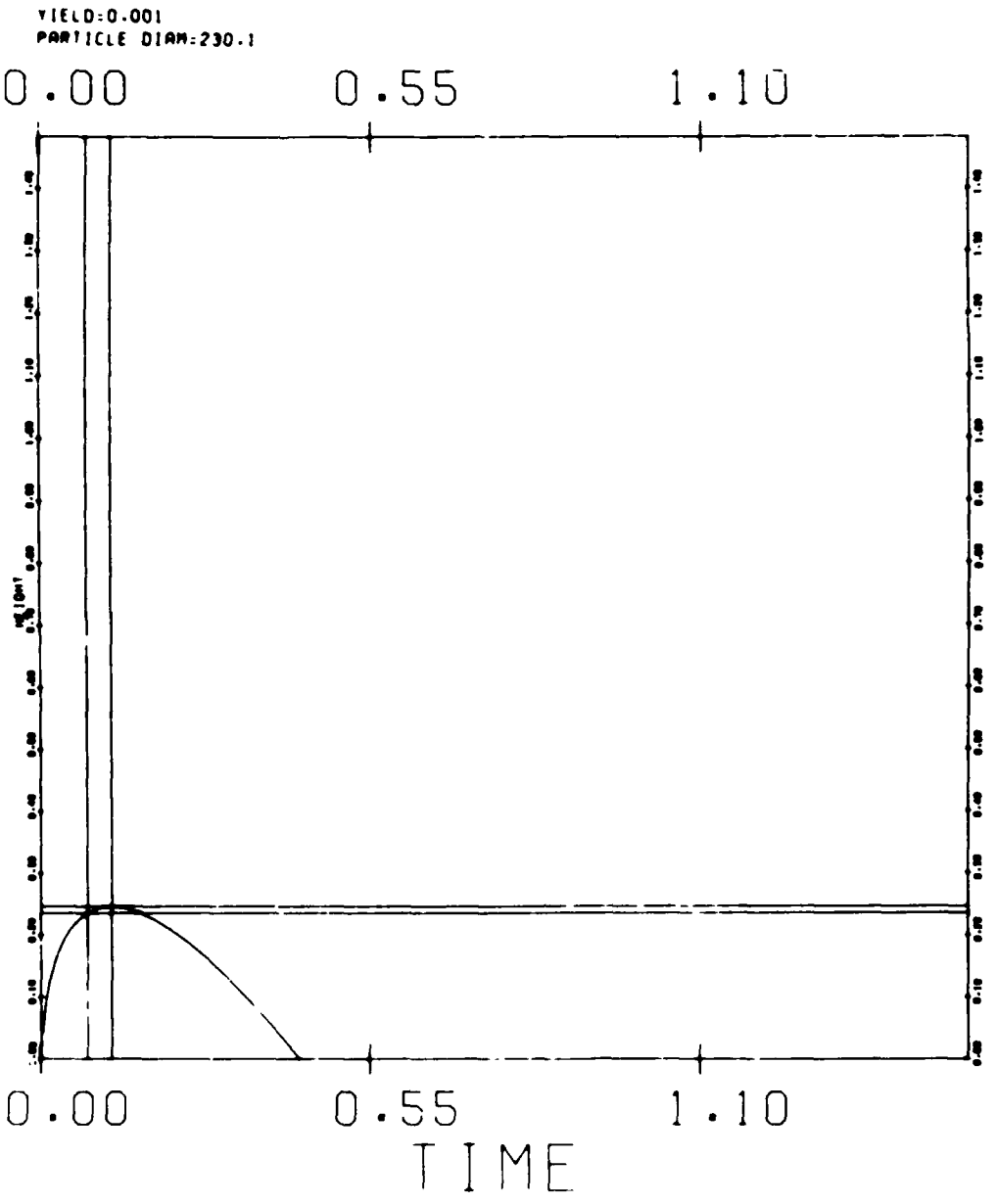

INITIALLY AT CLOUD BASE

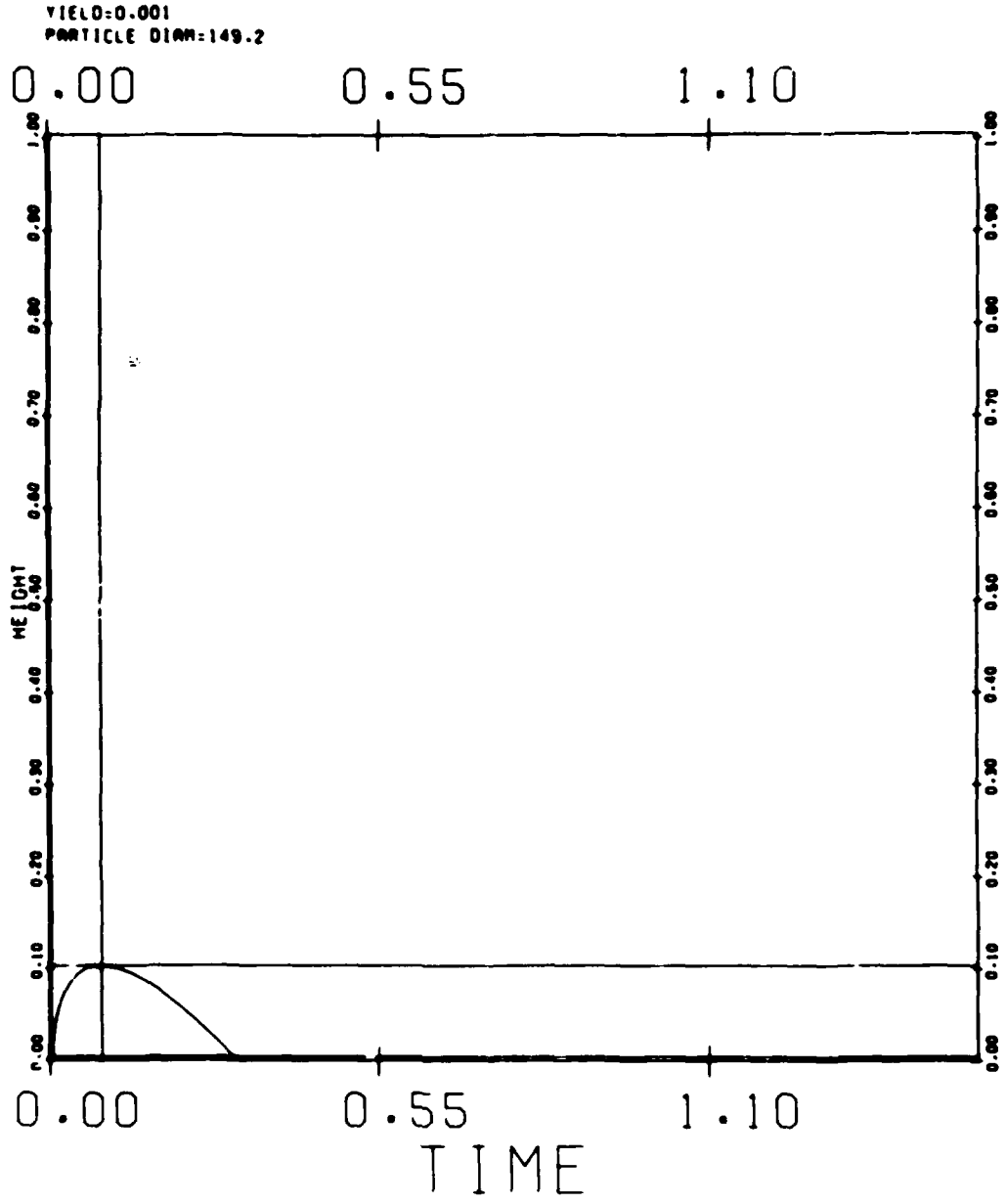

INITIALLY AT CLOUD TOP

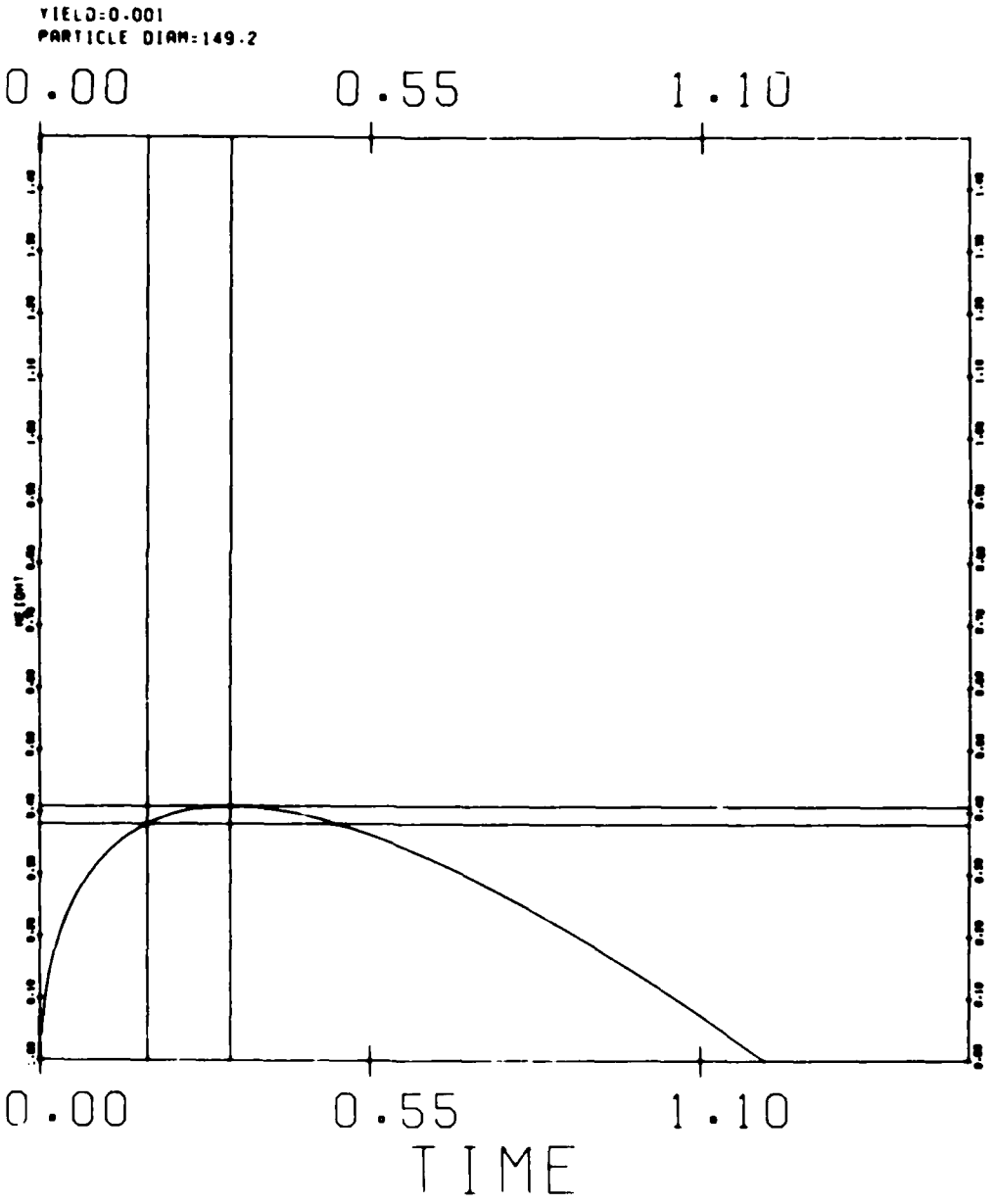

INITIALLY AT CLOUD BASE

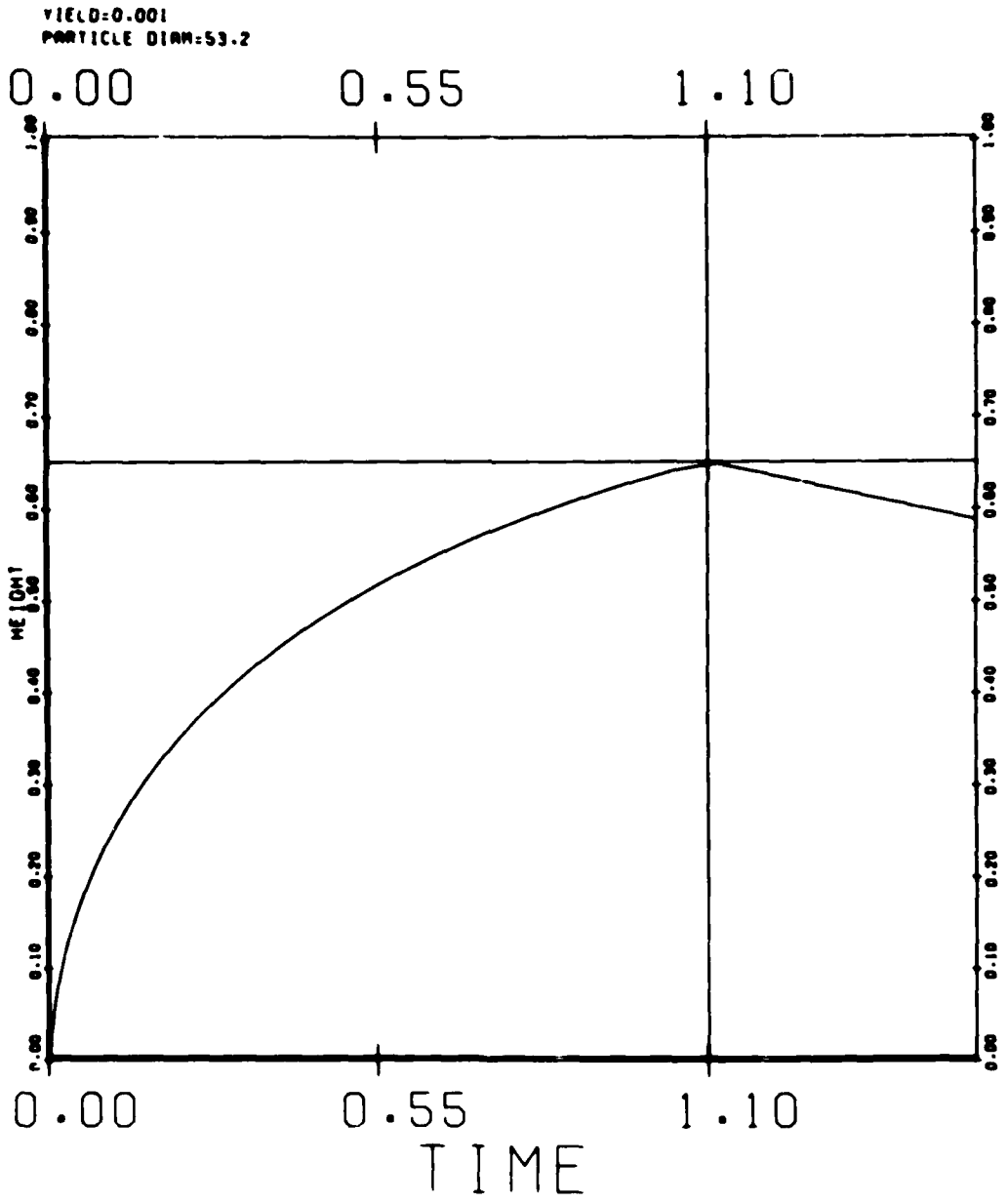

INITIALLY AT CLOUD TOP

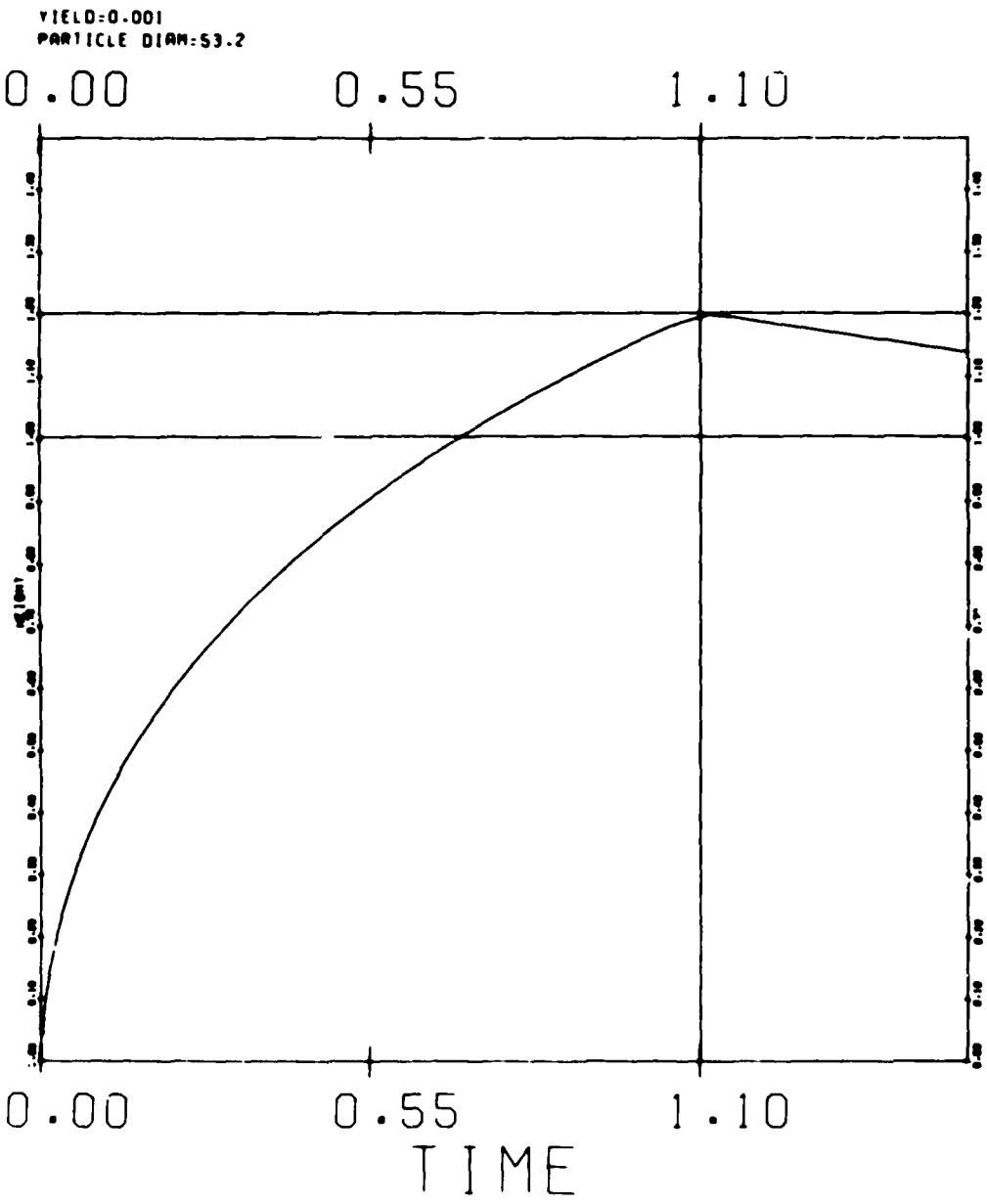

INITIALLY AT CLOUD BASE

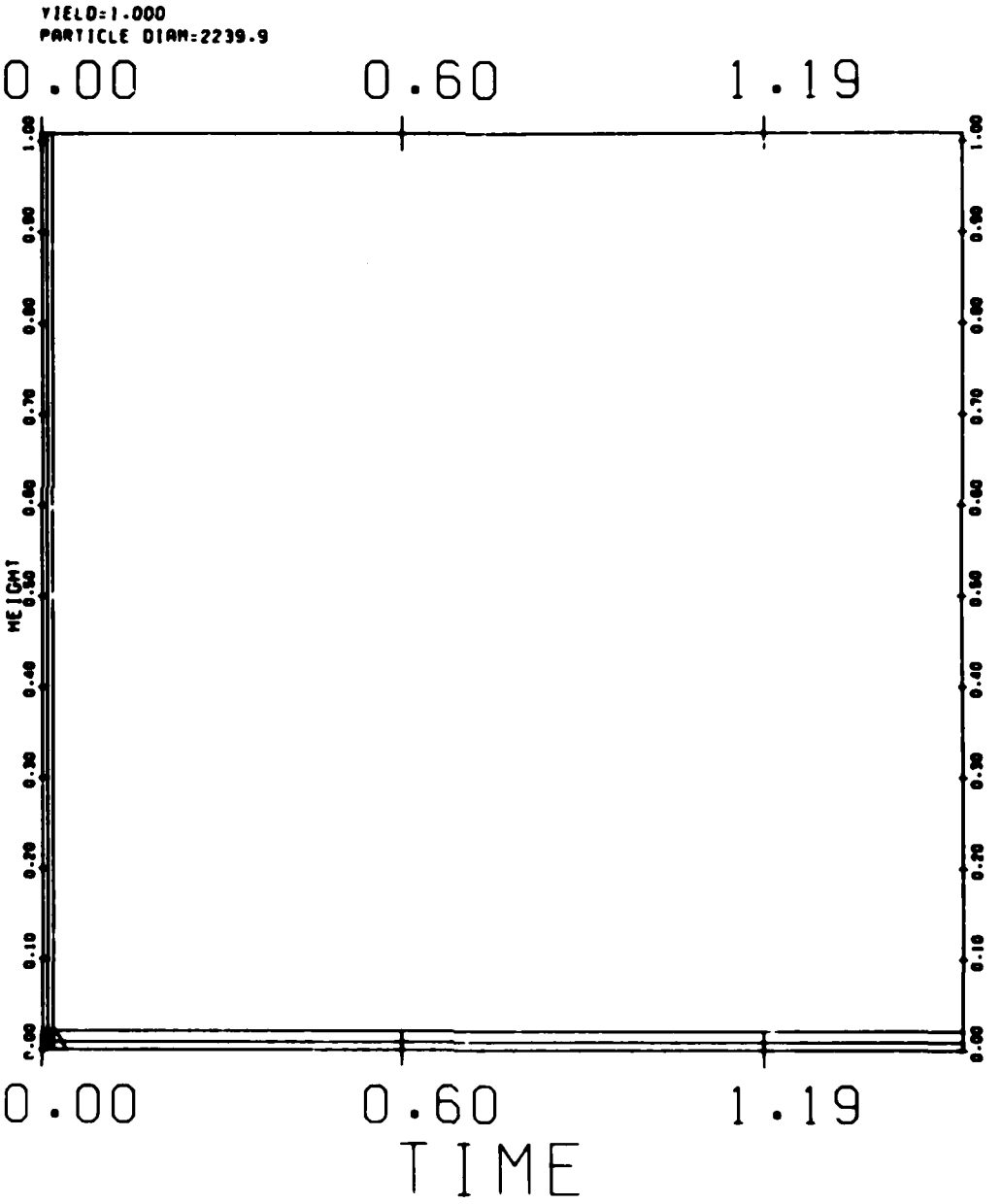

INITIALLY AT CLOUD TOP

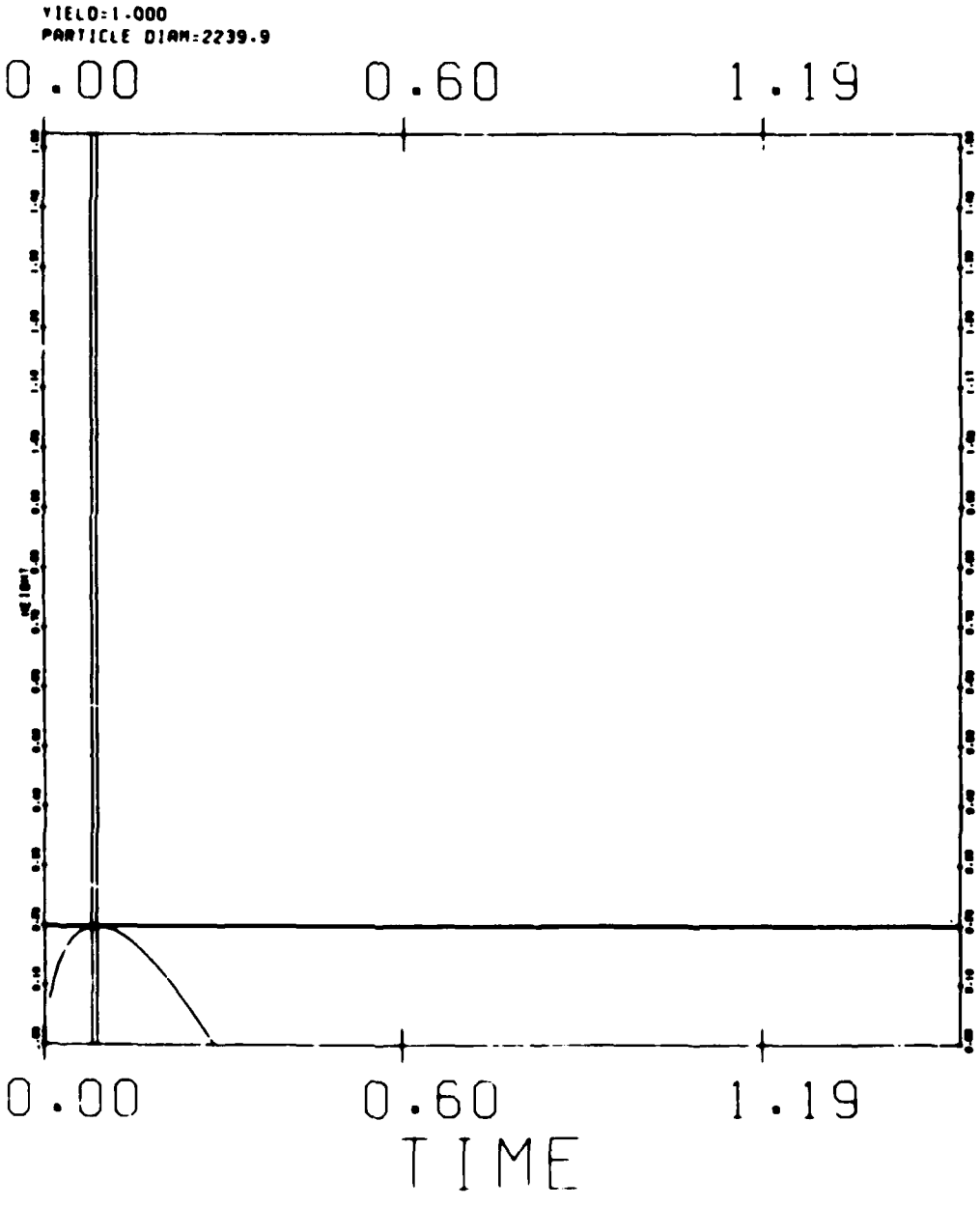

INITIALLY AT CLOUD BASE

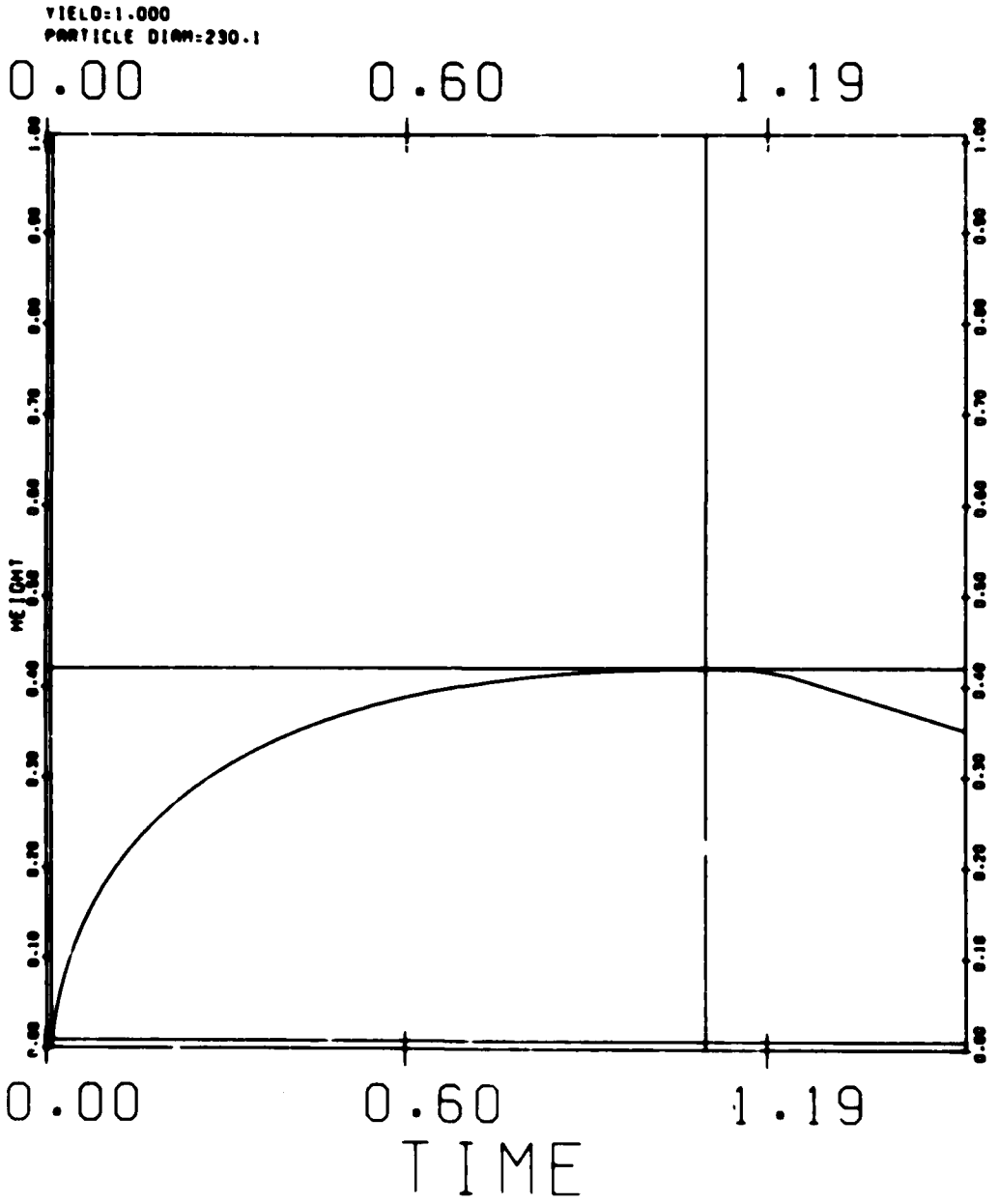

INITIALLY AT CLOUD TOP

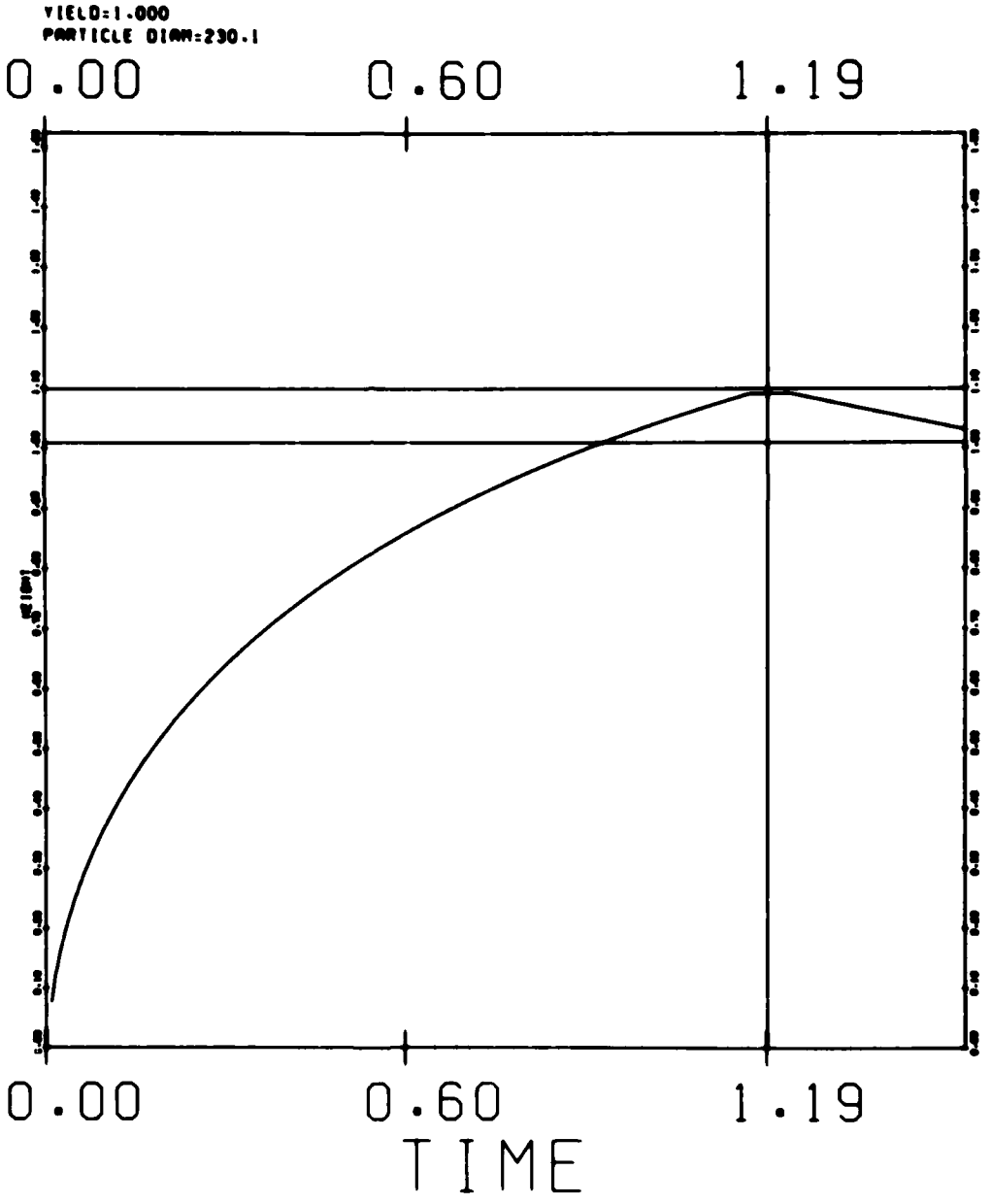

INITIALLY AT CLOUD BASE

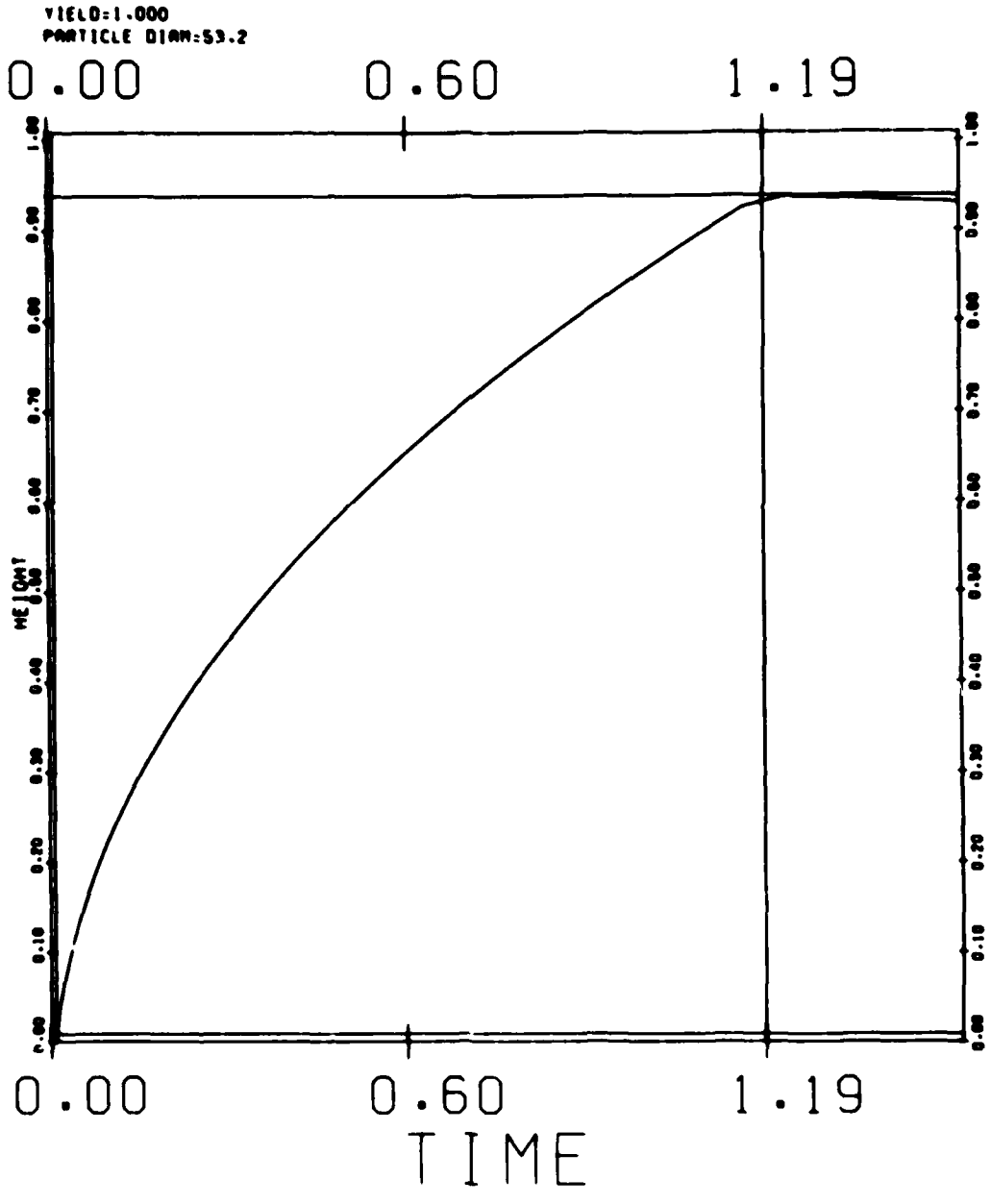

INITIALLY AT CLOUD TOP

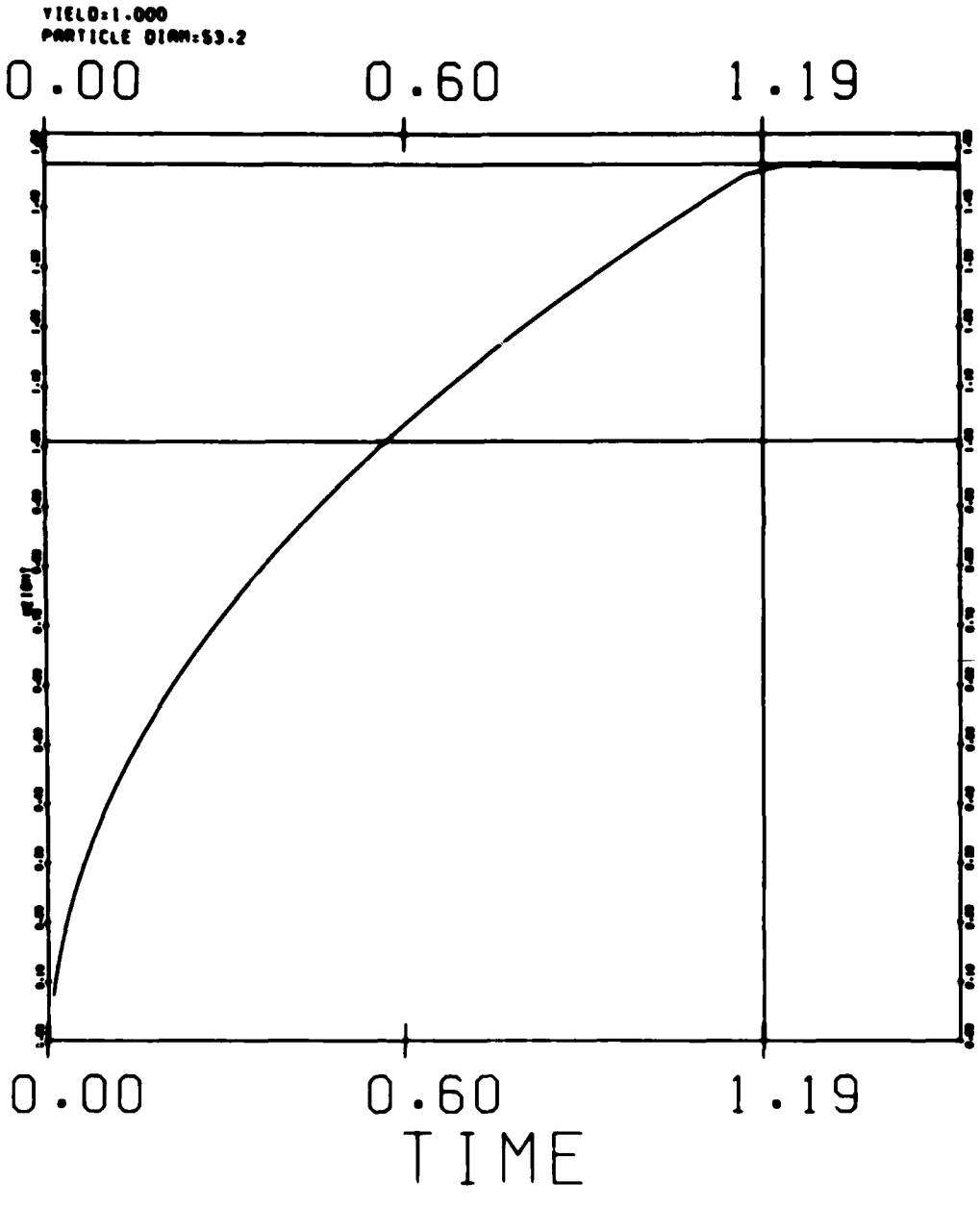

INITIALLY AT CLOUD BASE

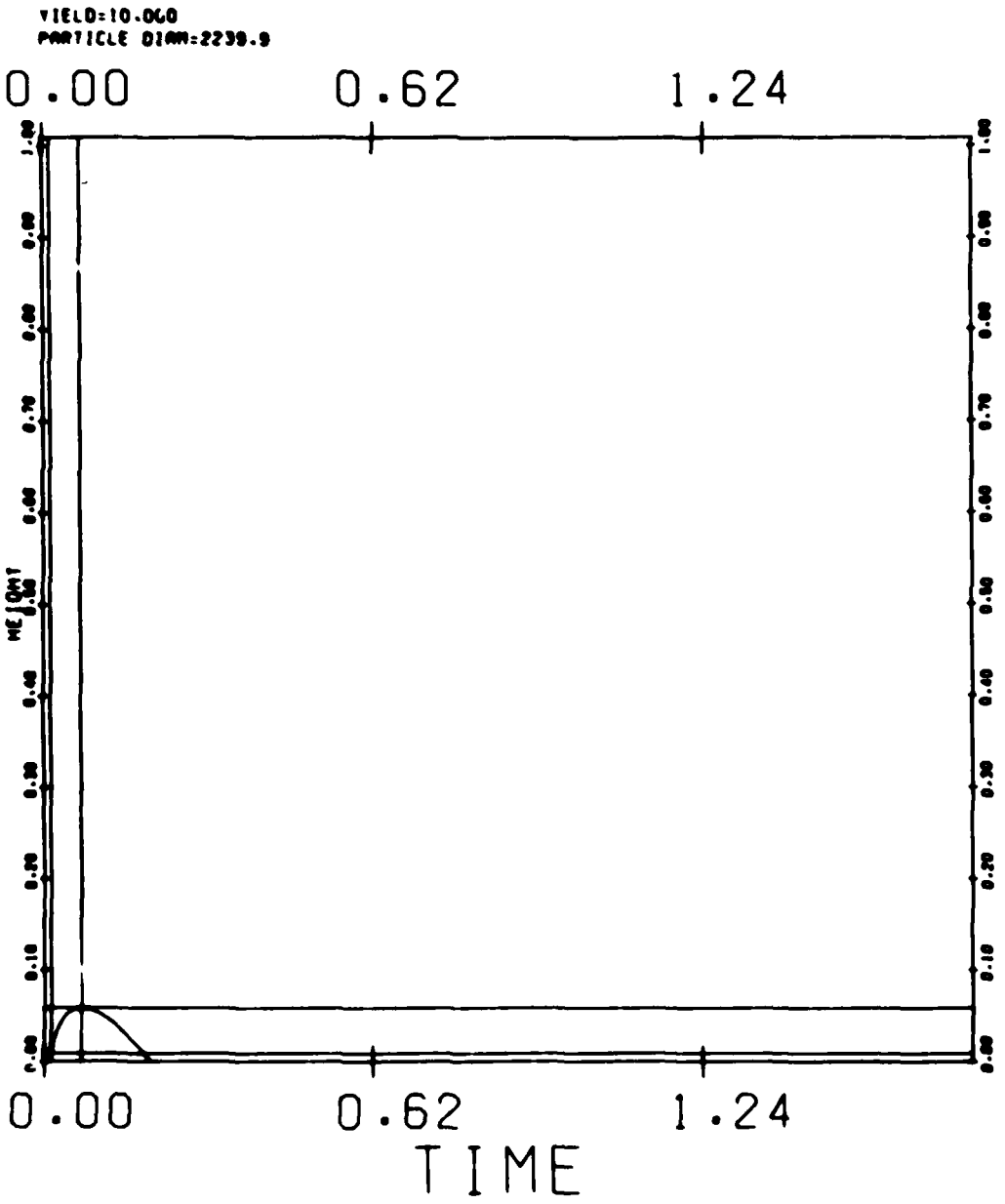

INITIALLY AT CLOUD TOP

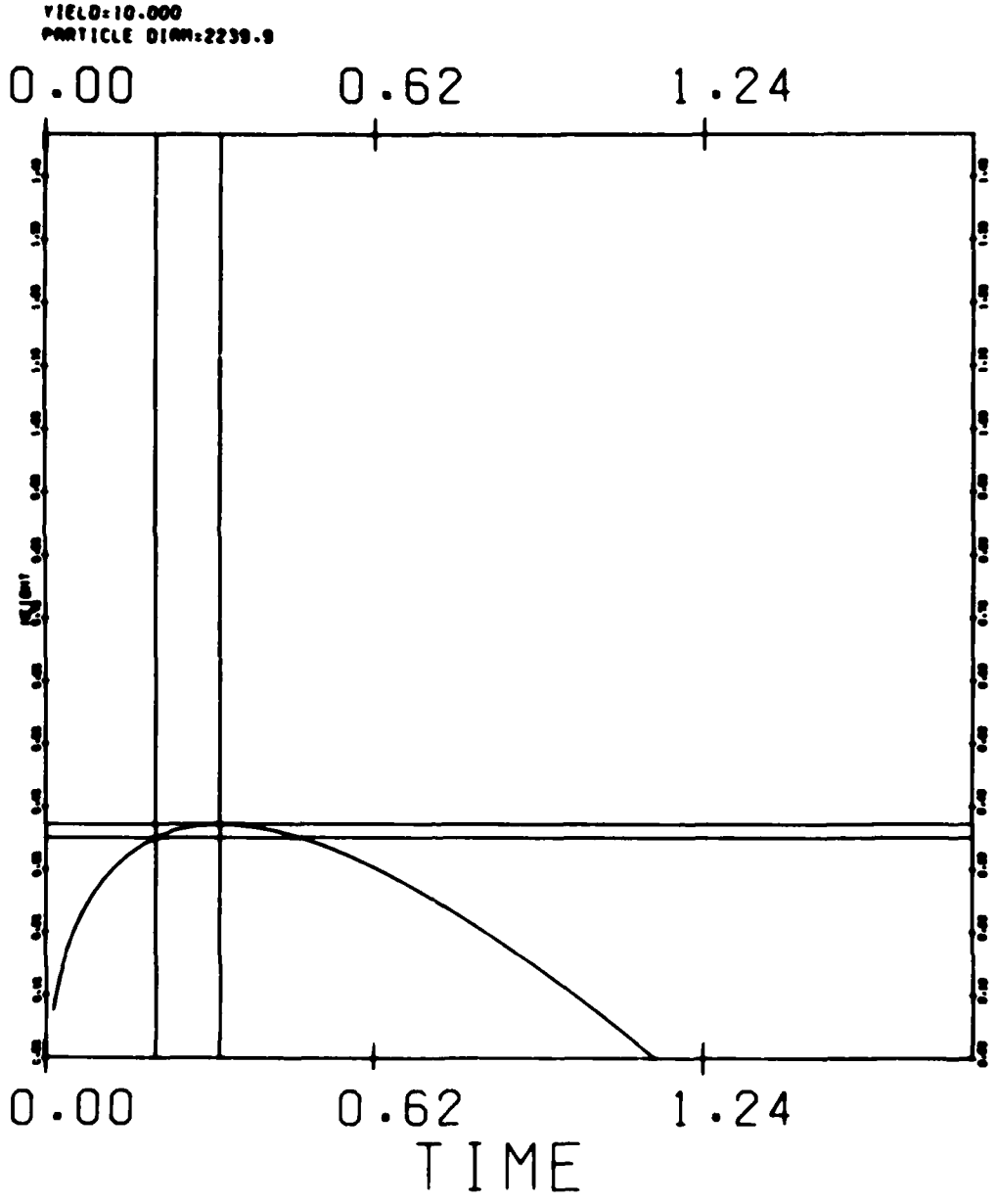

INITIALLY AT CLOUD BASE

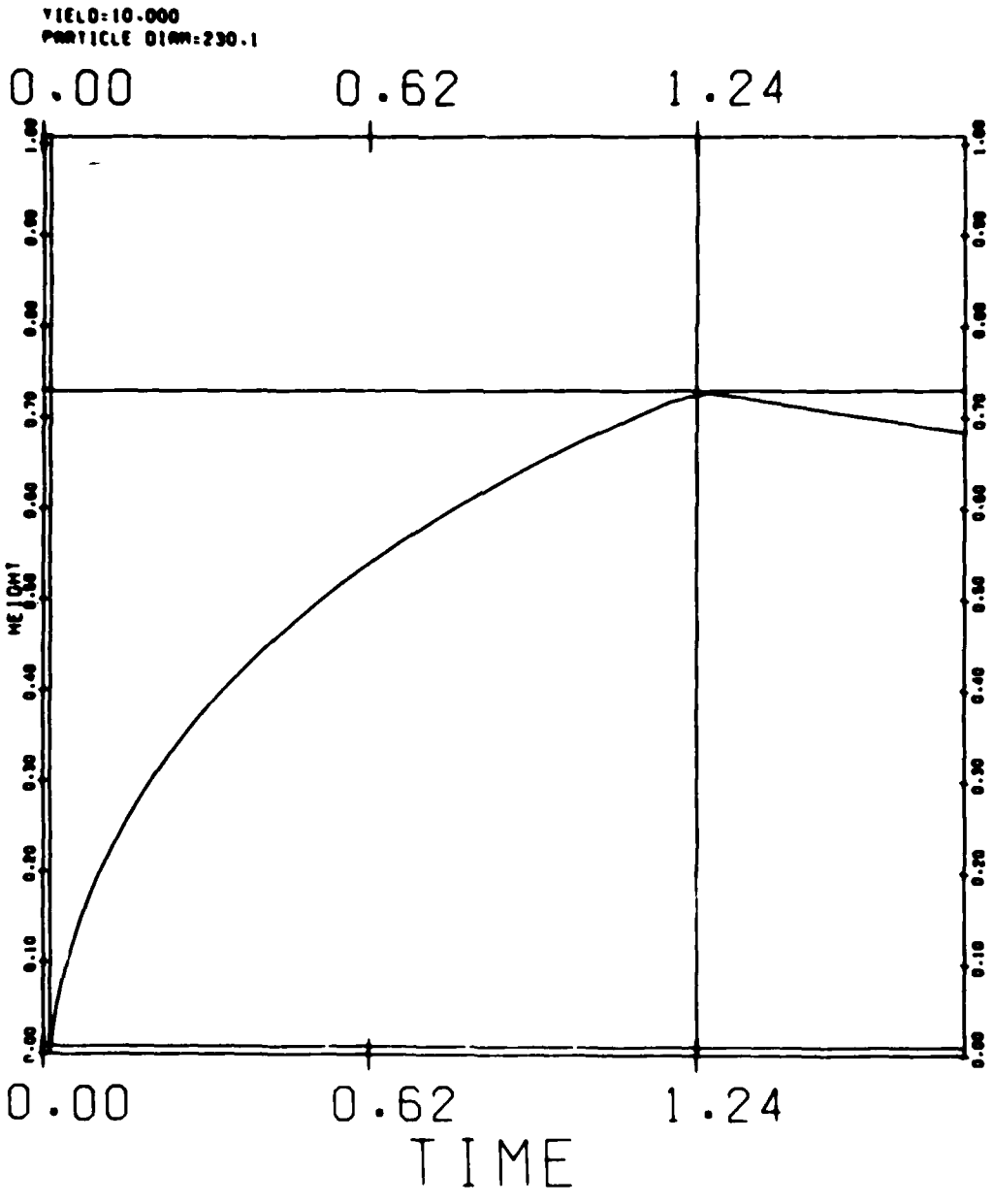

INITIALLY AT CLOUD TOP

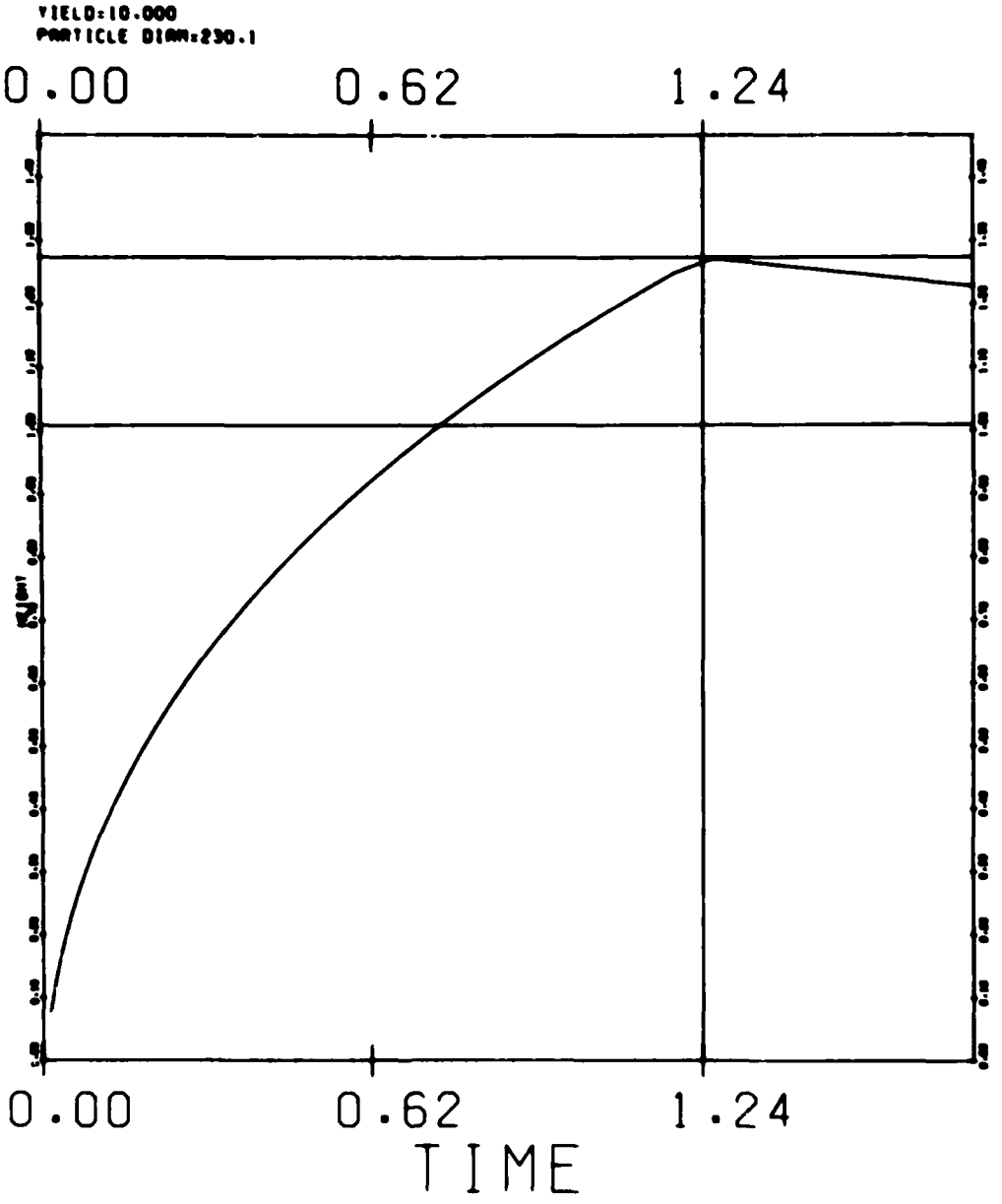

INITIALLY AT CLOUD BASE

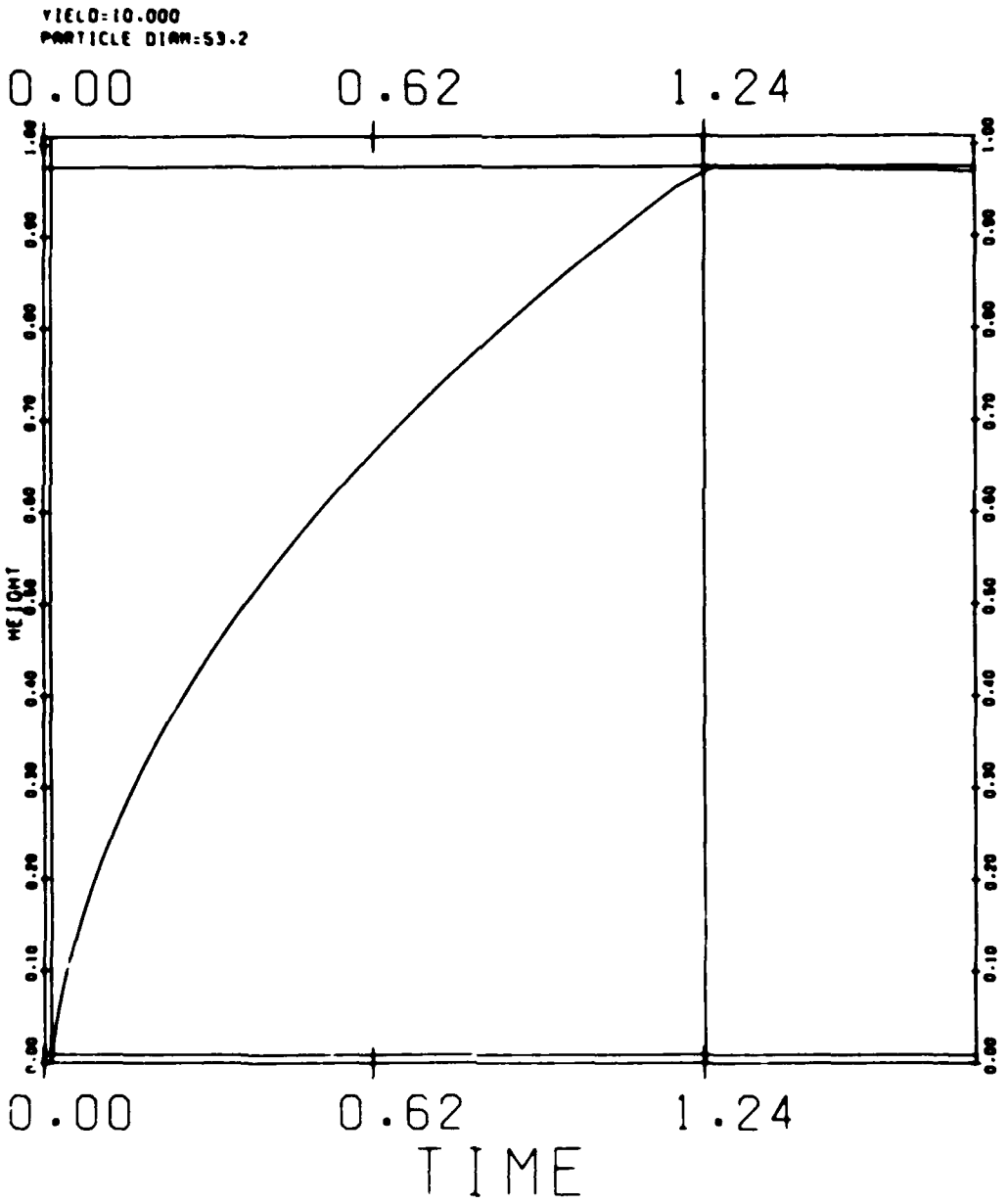

INITIALLY AT CLOUD TOP

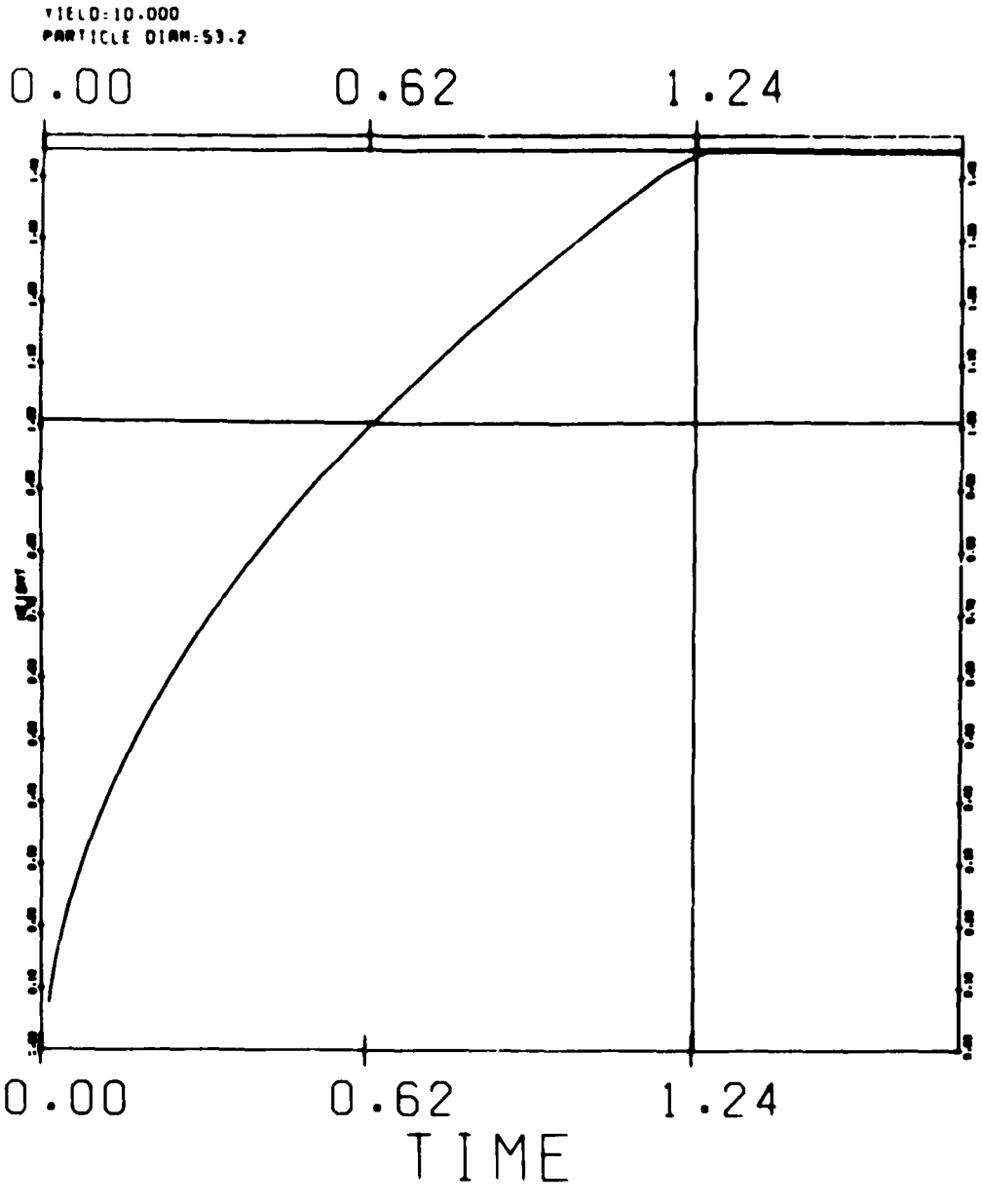

INITIALLY AT CLOUD BASE

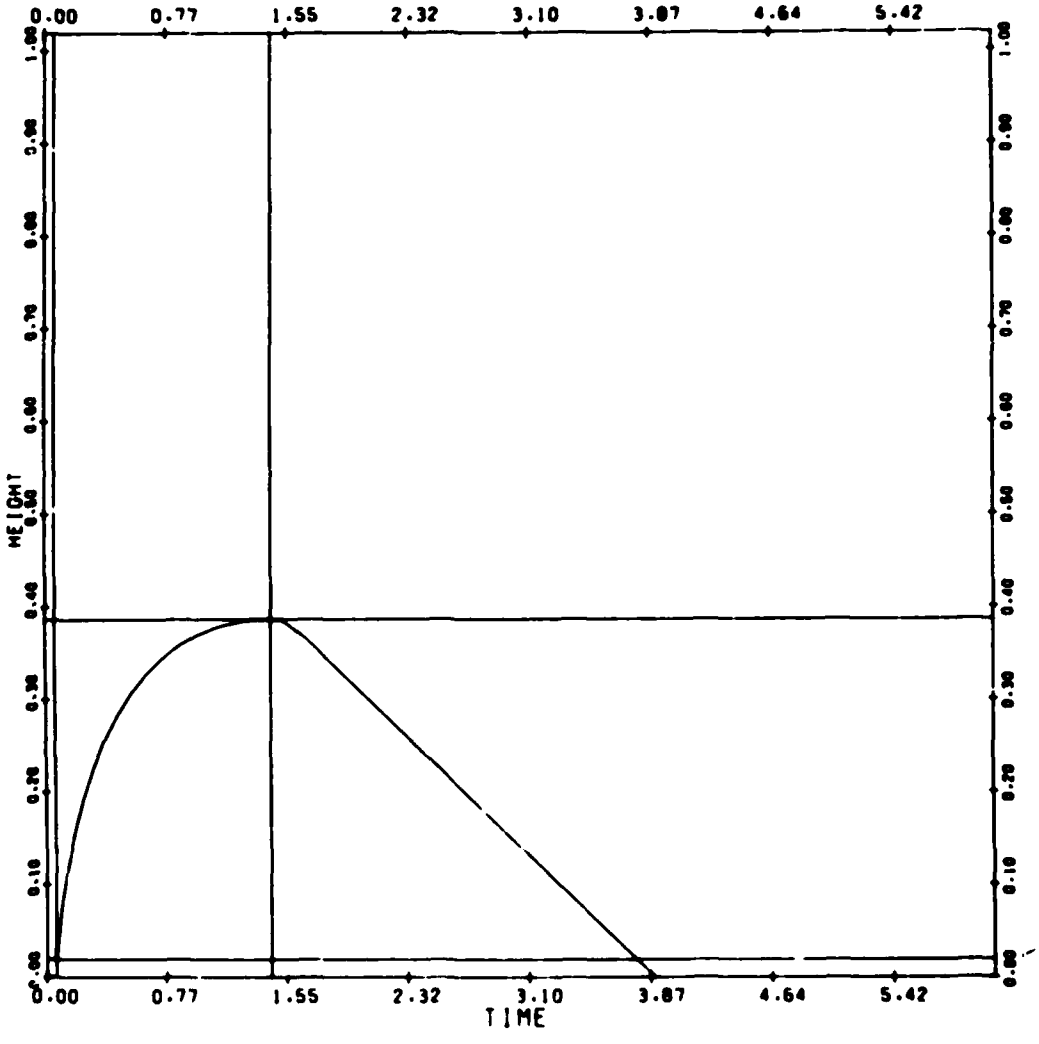

INITIALLY AT CLOUD TOP

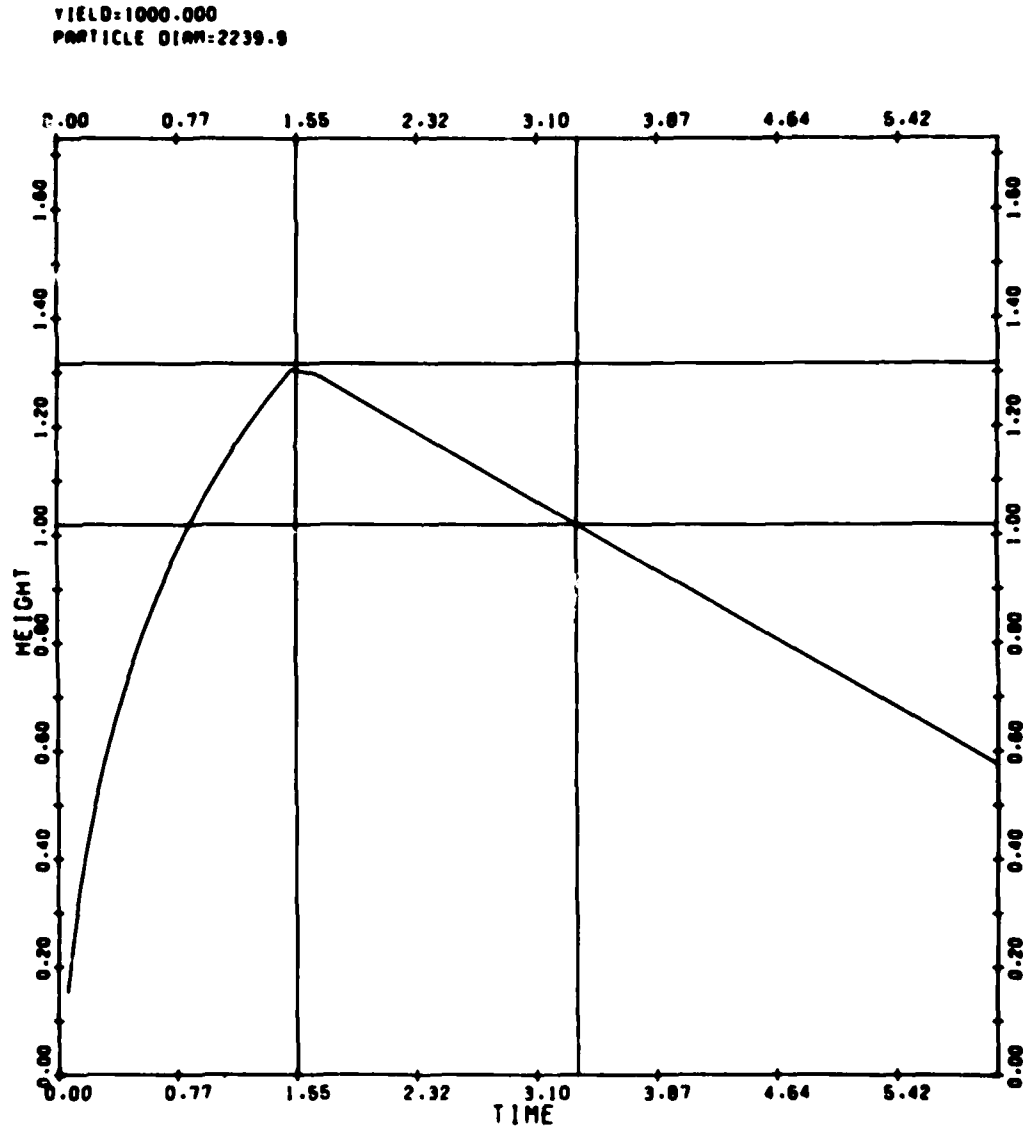

INITIALLY AT CLOUD BASE

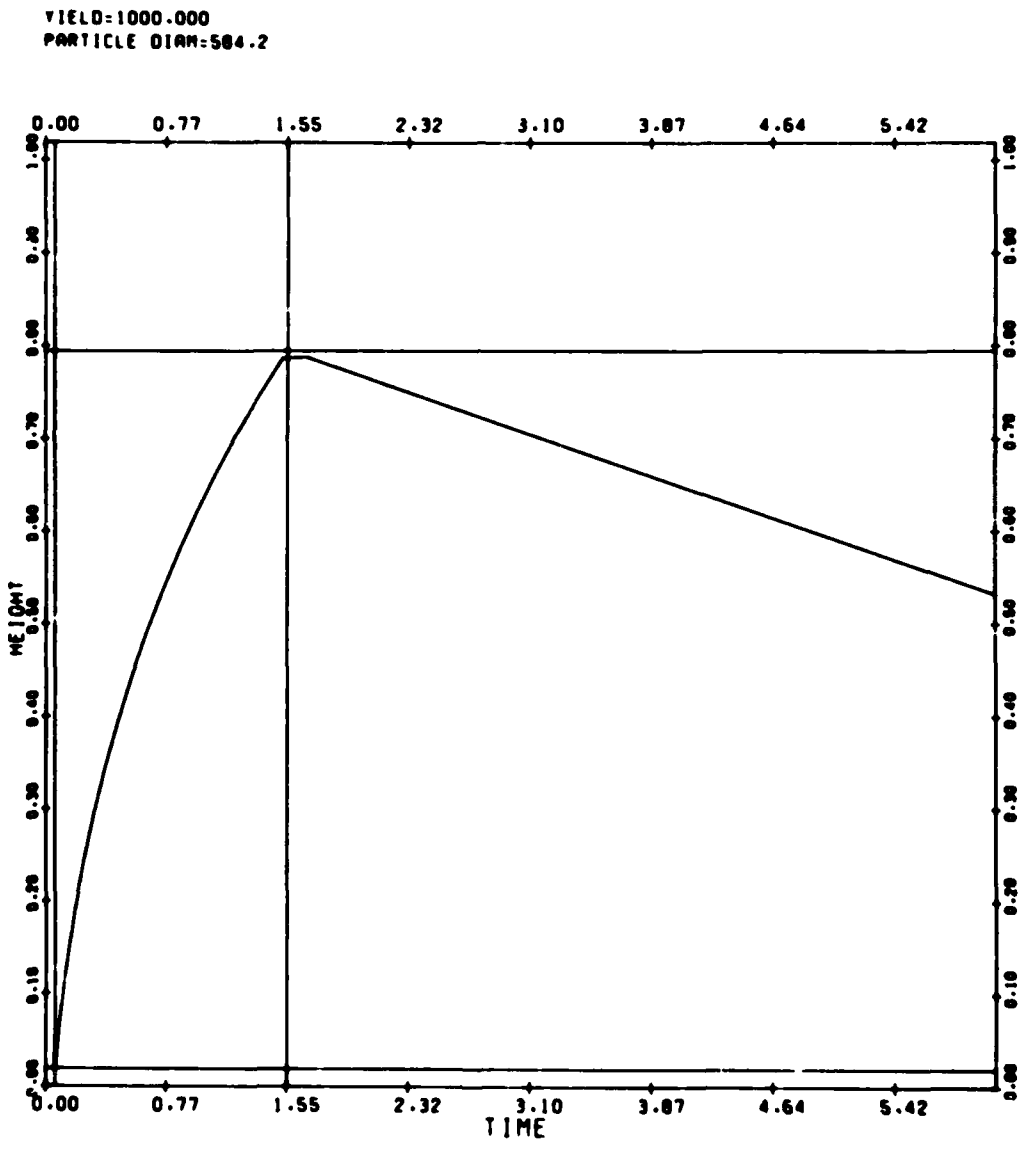

INITIALLY AT CLOUD TOP

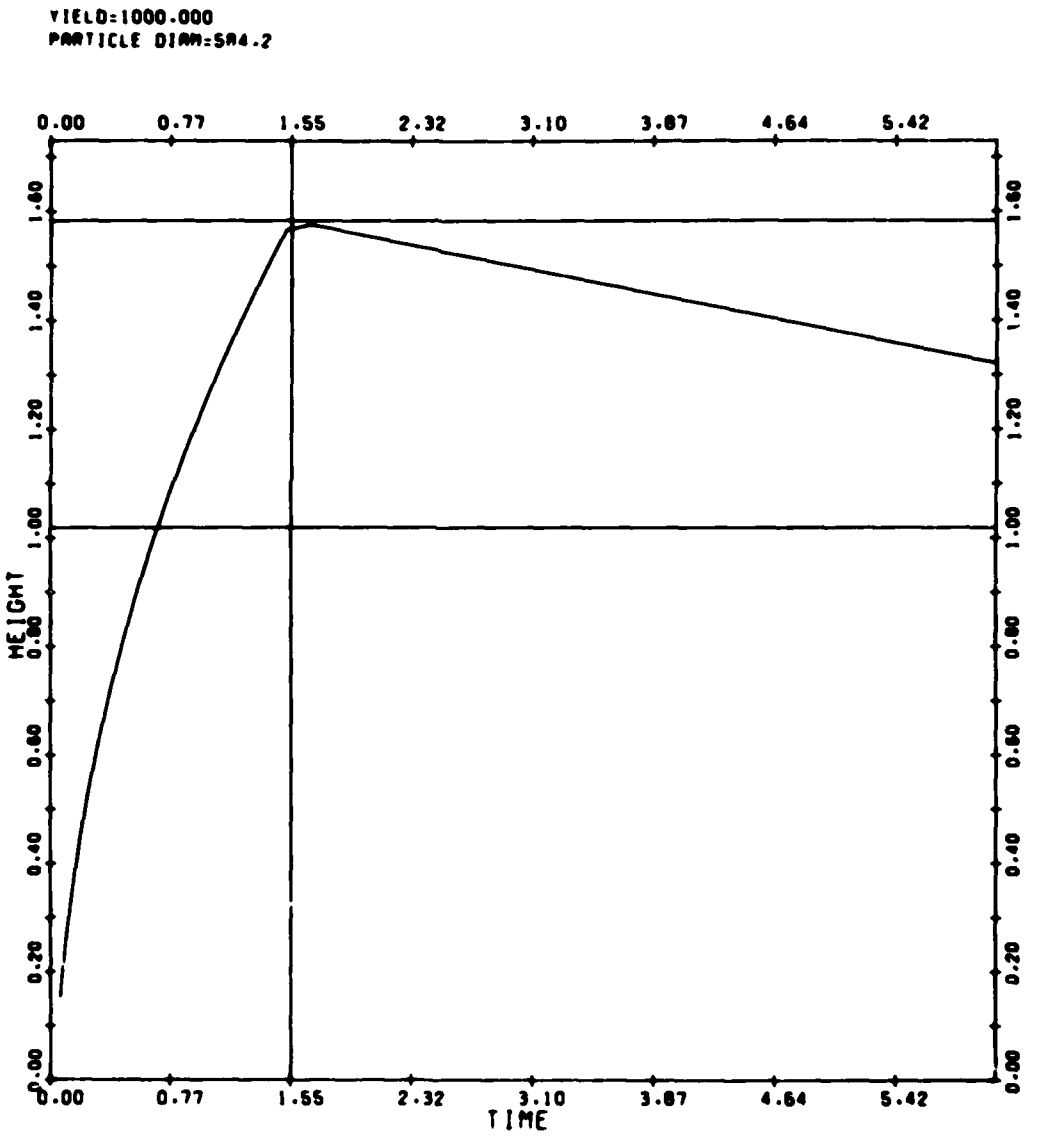

INITIALLY AT CLOUD BASE

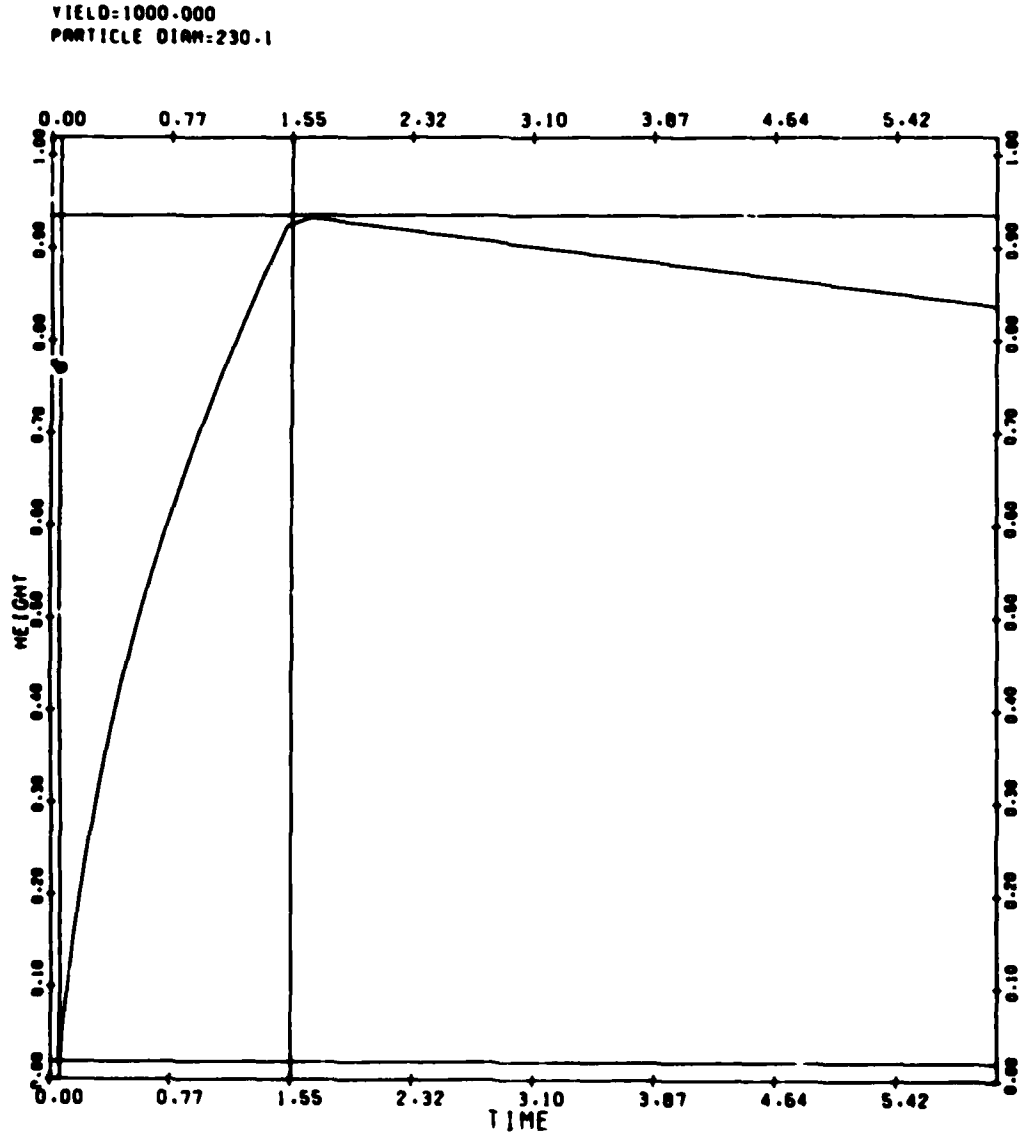

INITIALLY AT CLOUD TOP

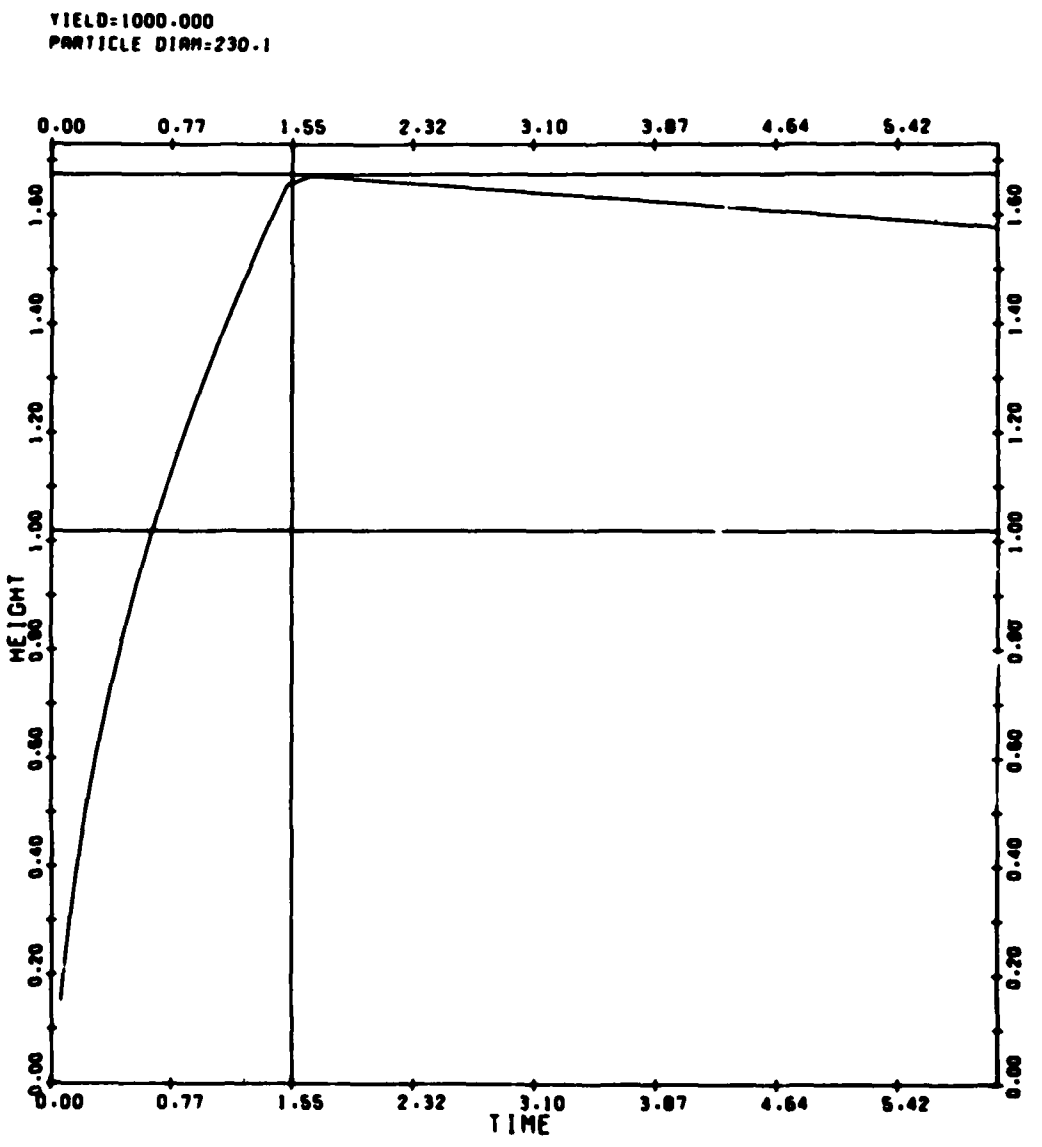

APPENDIX B

FALLOUT PATTERN COMPARISON BY THE FIGURE-OF-MERIT METHOD

Rowland and Thompson[19] developed this method for comparison of pairs of fallout contour maps by computation of a single index, the FM, that is a measure of contour overlap between them. For each contour common to the patterns, the area overlapped and the area not overlapped is calculated. The areas are weighted by the average radiation level between successive contours. Sums over all contours of weighted overlapped areas and weighted total areas are computed, and the FM is the ratio of the two sums. For completely overlapped, perfectly matched patterns, FM = 1; for no overlap, FM = 0.

Mathematically, FM is

$$FM = \frac{\sum_{i=1}^{N} \frac{(r_i + r_{i-1})}{2} (a_i - a_{i-1})}{\sum_{i=1}^{N} \frac{(r_i + r_{i-1})}{2} (A_i - A_{i-1})}$$

where

N is the number of contours in the patterns. The summations are from highest contour to lowest

r_i is activity of the i th contour (Roentgen/hr), $r_o = 10\ r_1$

a_i is common (i.e., overlapped) area for the i th contours. $a_o = 0$.

A_i is total area of the i th contour. The summation in the denominator is computed for both patterns, and the largest sum is used. $A_- = 0$.

The FM has been found to have limited utility as a measure of fallout prediction accuracy. This is mainly for two reasons. First, and most important, is that being a measure of overlap, the FM is strongly biased in favor of overprediction; that is, it favors predictions that cover a large area, and therefore overlap the observed pattern, regardless of other considerations. Second, the FM method imposes no penality for missing or extra contours; contours not common to both patterns are simply ignored.

DISTRIBUTION LIST

DEPARTMENT OF DEFENSE

Assistant to the Secretary of Defense
Atomic Energy
ATTN: T. Sisson

Command & Control Technical Center
ATTN: C-312, R. Mason

Defense Advanced Rsch. Proj. Agency
ATTN: TIO
ATTN: TTO

Defense Intelligence Agency
ATTN: DIO-GPF, W. Magathan
ATTN: DB-4C, P. Johnson
ATTN: RDS-3C
ATTN: DB-1, F. Walker
ATTN: DN
ATTN: DIR 4

Defense Nuclear Agency
ATTN: NATA
ATTN: RAAE
ATTN: STSP
ATTN: SPTD
ATTN: STNA
ATTN: STRA
ATTN: STSA
ATTN: RAEE
ATTN: NATD
4 cy ATTN: TITL

Defense Technical Information Center
12 cy ATTN: DD

Field Command
Defense Nuclear Agency
ATTN: FCP, J. DiGrazia
2 cy ATTN: FCPR

Field Command
Defense Nuclear Agency
Livermore Division
ATTN: FCPRL, L-395
ATTN: FCPRL

Field Command
Defense Nuclear Agency
Los Alamos Branch
ATTN: FCPRA

Interservice Nuclear Weapons School
ATTN: Document Control

Joint Chiefs of Staff
ATTN: SAGA/SFD
ATTN: SAGA/SSD
ATTN: J-5
ATTN: J-3

Joint Strat. Tgt. Planning Staff
ATTN: JL
ATTN: JP
ATTN: JPS
ATTN: JLTW

DEPARTMENT OF DEFENSE (Continued)

Undersecretary of Defense for Rsch. & Engrg.
ATTN: K. Hinman
ATTN: J. Morganstern

DEPARTMENT OF THE ARMY

Deputy Chief of Staff for Rsch. Dev. & Acq.
Department of the Army
ATTN: DAMA-CSM-N

Harry Diamond Laboratories
Department of the Army
ATTN: DELHD-N-TD
ATTN: DELHD-N-P
ATTN: DELHD-N-D
ATTN: Chairman, Nuc. Vulnerability Branch
ATTN: DELHD-I-TL

U.S. Army Armament Rsch. & Dev. Command
ATTN: DRDAR-LCN-E

U.S. Army Ballistic Research Labs.
ATTN: DRDAR-VL
ATTN: DRDAR-TSB-S
ATTN: DRDAR-BLV

U.S. Army Comd. & General Staff College
ATTN: Combined Arms Research Library

U.S. Army Concepts Analysis Agency
ATTN: MOCA-WG

U.S. Army Foreign Science & Tech. Ctr.
ATTN: DRXST-SD-I

U.S. Army Mobility Equip. R&D Cmd.
ATTN: DRDME-RT, K. Oscar
ATTN: DRDME-WC, Technical Library

U.S. Army Nuclear & Chemical Agency
ATTN: MONA-ZB, D. Panzer
ATTN: Library

U.S. Army War College
ATTN: Library

DEPARTMENT OF THE NAVY

Center for Naval Analysis
ATTN: NAVWAG

Naval Academy
ATTN: Nimitz Library/Tech. Rpts. Branch

Naval Postgraduate School
ATTN: Code 56PR
ATTN: Code 1424, Library

Naval Research Laboratory
ATTN: Code 8440, F. Rosenthal
ATTN: Code 2627

Naval Surface Weapons Center
ATTN: Code DG-50

DEPARTMENT OF THE NAVY (Continued)

Naval Surface Weapons Center
ATTN: Code R14
ATTN: Code U41
ATTN: Code F31
ATTN: Code U12
ATTN: Code F30

Naval War College
ATTN: Code E-11, Tech. Service

Naval Weapons Evaluation Facility
ATTN: Technical Director
ATTN: G. Binns

Office of Naval Research
ATTN: Code 431
ATTN: Code 200

DEPARTMENT OF THE AIR FORCE

Air Force Weapons Laboratory
Air Force Systems Command
ATTN: SUL
ATTN: NSSB

Assistant Chief of Staff
Studies & Analyses
Department of the Air Force
ATTN: AF/SAGF
ATTN: AF/SAMI
ATTN: H. Zwemer

Ballistic Missile Office
Air Force Systems Command
ATTN: NMR, R. Landers

DEPARTMENT OF ENERGY CONTRACTORS

Lawrence Livermore National Laboratory
ATTN: L-24, G. Staehle
ATTN: L-9, R. Barker
ATTN: L-21, M. Gustavson
ATTN: L-8, F. Barrish

Los Alamos National Scientific Laboratory
ATTN: R. Sandoval
ATTN: E. Chapin
ATTN: R. Stolpe
ATTN: W. Lyons
ATTN: M/S632, T. Dowler

Sandia National Laboratories
Livermore Laboratory
ATTN: T. Gold

Sandia National Laboratories
ATTN: J. Kaizur
ATTN: 3141

OTHER GOVERNMENT AGENCIES

Central Intelligence Agency
ATTN: OSR/SEC
ATTN: OSR/SE/F, A. Rehm
ATTN: OSI/NED

U.S. Arms Control & Disarmament Agcy.
ATTN: C. Thorn

OTHER GOVERNMENT AGENCIES (Continued)

Federal Emergency Management Agency
ATTN: Hazard Eval. & Vul. Red. Div.
ATTN: Deputy Director J. Nocita
ATTN: Asst. Dir. for Rsch., J. Buchanon

DEPARTMENT OF DEFENSE CONTRACTORS

Academy for Interscience Methodology
ATTN: N. Pointer

Atmospheric Science Associates
20 cy ATTN: H. Norment

BDM Corp.
ATTN: J. Braddock

Boeing Co.
ATTN: L. Harding

66th MI Group
ATTN: T. Greene

Decision-Science Applications, Inc.
ATTN: Dr. Pugh

General Electric Company—TEMPO
ATTN: DASIAC

General Electric Company—TEMPO
ATTN: DASIAC

Historical Evaluation & Rsch. Org.
ATTN: T. Dupuy

Hudson Institute, Inc.
ATTN: H. Kahn
ATTN: C. Gray

JAYCOR
ATTN: E. Almquist

Kaman Sciences Corp.
ATTN: V. Cox
ATTN: F. Shelton

Kaman Sciences Corp.
ATTN: T. Long

McLean Research Center, Inc.
ATTN: W. Schilling

Mission Research Corp.
ATTN: D. Sowle

Pacific-Sierra Research Corp.
ATTN: G. Lang

R&D Associates
ATTN: R. Montgomery
ATTN: C. MacDonald
ATTN: P. Haas

Rand Corp.
ATTN: Library
ATTN: T. Parker
ATTN: J. Digby

DEPARTMENT OF DEFENSE CONTRACTORS (Continued)

Santa Fe Corp.
ATTN: D. Paolucci
ATTN: N. Polmar
ATTN: E. Ortlieb
ATTN: M. Wade
3 cy ATTN: A. Billones

Science Applications, Inc.
ATTN: J. Goldstein
ATTN: J. McGahan
ATTN: W. Layson

DEPARTMENT OF DEFENSE CONTRACTORS (Continued)

SRI International
ATTN: B. Gasten
ATTN: J. Naar

System Planning Corp
ATTN: F. Adelman
ATTN: J. Douglas
ATTN: G. Parks